



# Ground-motion models for earthquakes occurring in the United Kingdom

John Douglas<sup>1</sup> · Guillermo Aldama-Bustos<sup>2</sup> · Sarah Tallett-Williams<sup>2</sup> ·  
Manuela Daví<sup>2</sup> · Iain J. Tromans<sup>2</sup>

Received: 1 February 2024 / Accepted: 22 May 2024  
© The Author(s) 2024

## Abstract

This article presents models to predict median horizontal elastic response spectral accelerations for 5% damping from earthquakes with moment magnitudes ranging from 3.5 to 7.25 occurring in the United Kingdom. This model was derived using the hybrid stochastic-empirical method based on an existing ground-motion model for California and a stochastic model for the UK that was developed specifically for this purpose. The model is presented in two consistent formats, both for two distance metrics, with different target end-users. Firstly, we provide a complete logic tree with 162 branches, and associated weights, capturing epistemic uncertainties in the depth to the top of rupture, geometric spreading, anelastic path attenuation, site attenuation and stress drop, which is more likely to be used for research. The weights for these branches were derived using Bayesian updating of *a priori* weights from expert judgment. Secondly, we provide a backbone model with three and five branches corresponding to different percentiles, with corresponding weights, capturing the overall epistemic uncertainty, which is tailored for engineering applications. The derived models are compared with ground-motion observations, both instrumental and macroseismic, from the UK and surrounding region (northern France, Belgium, the Netherlands, western Germany and western Scandinavia). These comparisons show that the model is well-centred (low overall bias and no obvious trends with magnitude or distance) and that the branches capture the body and range of the technically defensible interpretations. In addition, comparisons with ground-motion models that have been previously used within seismic hazard assessments for the UK show that ground-motion predictions from the proposed model match those from previous models quite closely for most magnitudes and distances. The models are available as computer subroutines for ease of use.

**Keywords** Ground-motion models (GMMs) · Ground motion prediction equations (GMPEs) · Backbone method · Stochastic method · Hybrid empirical-stochastic method · United Kingdom (UK)

---

✉ John Douglas  
john-douglas@gmx.com

<sup>1</sup> Department of Civil and Environmental Engineering, University of Strathclyde, James Weir Building, 75 Montrose Street, Glasgow G1 1XJ, UK

<sup>2</sup> Jacobs, Cottons Centre, Cottons Lane, London SE1 2QG, UK

## 1 Introduction

Due to its distance from active plate boundaries, the United Kingdom<sup>1</sup> lies within a region of low to moderate seismic hazard. It is generally classified (e.g. Schulte and Mooney 2005; Delavaud et al. 2012) as being in a stable continental region (SCR). Nevertheless, the amplitudes of earthquake ground motions observed in the UK appear to lie somewhere between those from active crustal regions (ACRs) and those from SCRs (e.g. Villani et al. 2019), although there is considerable uncertainty over exactly where they lie due to the lack of recordings from earthquakes with moment magnitude ( $M$ ) above 5.0. Recent seismic hazard assessments for the UK, including for critical infrastructure (e.g. nuclear power plants), have generally used a suite of ground motion prediction equations (GMPEs) from both ACRs and SCRs as well as UK-specific models (e.g. Tromans et al. 2019; Villani et al. 2020; Mosca et al. 2022; Aldama-Bustos et al. 2023). Adjusting models from other regions (e.g. the Mediterranean area, California or eastern North America) is associated with large and difficult-to-quantify uncertainties. These uncertainties can lead to significant challenge to using adopted/adjusted models, for example in the highly regulated nuclear sector.

Recent UK-specific models (Rietbrock et al. 2013; Rietbrock and Edwards 2019) were assigned low weights within the ground-motion logic trees of recent UK seismic hazard studies because of doubts about the applicability of these models to magnitudes and distances outside the range of available instrumental observations, which are generally from  $M < 5.0$  and epicentral distances ( $R_{\text{epi}}$ ) greater than 50 km. Disaggregation of seismic hazard results for typical UK sites show that the key earthquake scenarios are generally from shorter distances ( $R_{\text{epi}} < 50$  km) and larger magnitudes ( $M > 5.0$ ) (e.g. Goda et al. 2013; Tromans et al. 2019; Mosca et al. 2022).

The ground-motion models (GMMs) presented here are derived using the hybrid stochastic-empirical method (HEM) (Campbell 2003) and the backbone philosophy (Atkinson et al. 2014), which has been increasingly used in the nuclear sector over the past decade. The backbone approach, where a logic tree is populated with scaled versions of a single model, enables epistemic uncertainties to be transparently and rigorously captured by means of a logic tree with appropriate weights (e.g. Douglas 2018; Bommer and Stafford 2020; Bommer 2024). In the alternative, multi-GMPE, approach, which has often been adopted within UK seismic hazard assessments, the epistemic uncertainty captured by the GMM is not controlled by design but is an indirect consequence of the GMPE choice and weights. In addition, each GMPE needs to be adjusted individually to the site of interest, which can be challenging because, for example, the average shear-wave velocity profile consistent with the GMPE is often unknown. Adopting the backbone philosophy to develop the models should make their adaptation to a specific site easier.

Developing GMMs for the UK presents several challenges, many of which are common to other regions of low-to-moderate seismicity (e.g. much of Europe outside the Mediterranean region). Firstly, the depth range of earthquakes with  $M > 5.0$  is poorly known as most estimates for this magnitude range are from macroseismic intensities and not instrumental data. Secondly, as mentioned above there is a lack of data for the hazard critical magnitude-distance range. Thirdly, the useful frequency range of data that are available is limited due

<sup>1</sup> Because of the very low seismicity of Northern Ireland, the ground-motion models developed here are focussed on Great Britain rather than the whole of the UK, but we use the UK as a convenient shorthand.

to low signal-to-noise ratios for  $< 1$  Hz and  $> 10$  Hz. Fourthly, there is limited information available on the local site conditions at seismic stations contributing ground-motion records, which makes it difficult to adjust them to a common reference. Fifthly, the shear-wave velocity structure of the near-surface (depth  $< 2$  km) is poorly known, which makes host-to-target adjustments (e.g. Al Atik et al. 2014) subject to large uncertainties. In the following sections, methods we have implemented to overcome these difficulties are discussed.

The following section outlines the method used to derive the GMMs. Section 3 presents the UK stochastic models developed in this study. The subsequent section compares the resulting GMM branches against instrumental data and uses these data to update the *a priori* weights assigned to each branch. In addition, to facilitate the use of the model within hazard assessments, a backbone formulation of the model with fewer branches is also presented in Sect. 4. In Sect. 5, predictions from the models are compared to GMMs commonly used in previous UK seismic hazard assessments. The article ends with a brief summary and application guidelines for the GMM.

## 2 Methods

In this section, the method followed to develop the GMMs is discussed. The approach is based on the HEM proposed by Campbell (2003) and uses a modified version of the CHEEP software from Douglas et al. (2006) to implement this method. This method uses the ratios between stochastic models (e.g., Boore 2003) for host and target regions to adjust an empirical GMM for the host region to make it applicable to the target region (here the UK). The host empirical and stochastic models chosen are discussed in the next subsection and the main methodology decisions are summarised in Table 1.

The stochastic models for the target region should capture appropriate epistemic uncertainties. These uncertainties are generally larger for the target region than for the host region because of fewer ground-motion records, which are generally of small ( $M < 5.0$ ) earthquakes recorded at large ( $R_{\text{epi}} > 100$  km) distances. A suite of stochastic models was developed specifically for the UK as part of this study (see Sect. 3); these models are key inputs to the HEM.

### 2.1 Host empirical and stochastic models

The Chiou and Youngs (2014) GMPE, which was developed using California data supplemented, at large magnitudes, by data from other ACRs globally (e.g. Taiwan, Italy and Japan), was chosen as the host empirical model for a number of reasons. Firstly, this GMPE is recommended by its developers for the entire magnitude range of interest to the UK (here assumed to be  $M$  3.5 to  $M$  7.25) and distances up to 300 km, which is the maximum distance generally used for seismic hazard assessments for UK sites (e.g. Tromans et al. 2019). Secondly, the GMPE provides coefficients for periods between 0 and 10 s, again covering the period range of interest to this study. Thirdly, Bommer and Stafford (2020) recommend this model for its “adaptability”, as its functional form captures the magnitude and distance scaling expected by seismological theory and isolates the influence of source and path parameters. Finally, Stafford et al. (2022), using the  $V_S$  profile and kappa estimates from Al Atik and Abrahamson (2021), develop a stochastic model that provides predicted ground motions that closely match the empirical estimates of Chiou and Youngs (2014).

**Table 1** Summary of modelling decisions and key considerations for methodology

Model element	Decision	Key considerations
Overall approach	Hybrid empirical method	Lack of UK data Used in several previous studies Does not require lots of inputs
Host empirical model	Chiou and Youngs (2014)	GMPE had sufficient magnitude range, distance range and response periods Recommended by Bonner and Stafford (2020) Closely matched by Stafford et al. (2022) stochastic model
Host Stochastic model	Stafford et al. (2022)	Close match to Chiou and Youngs (2014) Ease of implementation in SMSIM software
Style of faulting	Vertical strike slip faulting (SS)	Chiou & Youngs (2014) database is chiefly SS Baptie (2010) demonstrates UK faulting is mainly SS
$Z_{TOR}$	Chiou and Youngs (2014) for host Two UK specific models	UK focal depths indicate different distribution than in California Uncertainty over correct model
Magnitude range	$M$ 3.5–7.25	Widest range of potential interest for UK Simulation of data from $M$ 3.0–7.75 to avoid edge effects
Distance range	0–1000 km	Widest range of engineering interest Allows validation against other UK data
Spectral period and damping	0.01 s (PGA) to 10.0 s at 5% damping	Widest range of engineering interest Standard damping ratio
Software	CHEEP SMSIM	Easily adaptable to produce results for both empirical and stochastic models

Thanks to the study by Stafford et al. (2022), and the use of this model in a seismic hazard assessment for the Idaho National Laboratory (Boore et al. 2022), this model is included within the version of the software (from 3rd March 2023<sup>2</sup>) used to implement the stochastic method, SMSIM (Stochastic-Method SIMulation) (Boore 2005). Boore et al. (2022) note that the Chiou and Youngs (2014) GMPE predicts lower long-period ( $T > 2$  s) response spectral accelerations than other NGA-West2 GMPEs, and they develop an empirical adjustment for this. If response spectral accelerations for  $T > 2$  s are of particular interest to users of the GMM presented here, then they are recommended to consider adopting this empirical adjustment. Nevertheless, the period range of most applications of this GMM is likely  $T \leq 2$  s and hence we do not consider this adjustment here.

The “optimal” implementation of Stafford et al. (2022), which uses 13 free parameters, captures the observed magnitude dependency of the exponent of Q and employs two distance metrics, is adopted because it provides the best overall fit to the empirical predictions of Chiou and Youngs (2014). Comparisons presented by Stafford et al. (2022) show that the host stochastic and empirical models deviate at longer periods ( $T > 1$  s) for large magnitudes ( $M > 6.5$ ), which is due to the assumption of a single-corner source spectrum by Stafford et al. (2022). When predictions from the host stochastic ( $S_{host}$ ) and empirical ( $E_{host}$ ) models match exactly, the target “empirical” model ( $E_{target}$ ) equals the target stochastic ( $S_{target}$ ) model (as the adjustment factor, i.e. the ratio of the host empirical to stochastic predictions,  $E_{host}/S_{host}$ , becomes unity). It was confirmed (see Electronic Supplement) that  $E_{target} \approx S_{target}$  i.e. the target “empirical” and the target stochastic predictions match except for  $T > 1$  s and  $M > 6.5$ . For  $T > 1$  s and  $M > 6.5$ , the use of the empirical model leads to more realistic predictions because it corrects for limitations in the single-corner spectral shape used for the stochastic models.

Vertical strike-slip faulting earthquakes for both the host and target regions are assumed for simplicity. This assumption is also justified by observing that the model of Chiou and Youngs (2014) was derived using considerable data from strike-slip events and since Baptie (2010) demonstrated that strike-slip faulting is the dominant style of faulting in the UK. The  $Z_{TOR}$  model proposed by Chiou and Youngs (2014) and used by Stafford et al. (2022) to derive their stochastic characterisation of this empirical model is used when generating the empirical and stochastic estimates for the host region. In addition, the rupture distances,  $R_{RUP}$ , are converted to point-source distances,  $R_{PS}$ , for use in the stochastic model via Eqs. 1 and 2 for ACRs from Boore and Thompson (2015). The Boore and Thompson (2015) proposal for SCRs is not used for the UK as it is not clear that UK events have a larger stress drop than events in ACRs (see below).

## 2.2 Generation of the model

The Fortran program CHEEP, which was developed by Douglas et al. (2006) to implement the HEM for two case studies (southern Norway and southern Spain), was the basis of the process used to generate the HEM for the UK. The original version of CHEEP, however, did not include the Chiou and Youngs (2014) model as one of its built-in host empirical models. This model was added to CHEEP, but it proved infeasible to incorporate into CHEEP the stochastic model developed by Stafford et al. (2022) to match this empirical model. This was because CHEEP used SMSIM (Boore 2005) subroutines from its 2003 version, while evaluating the

<sup>2</sup> [https://daveboore.com/software\\_online.html](https://daveboore.com/software_online.html)

stochastic model of Stafford et al. (2022) required the most recent version of SMSIM (from 2023). A workaround for this problem was implemented. This consisted of running CHEEP for one of its built-in stochastic models and then post-processing the output files to update all the stochastic estimates with those computed by the latest version of SMSIM and the Stafford et al. (2022) optimal parameterisation.

We aim to develop a GMM to be used from  $M$  3.5 to the largest earthquakes that are considered in seismic hazard analysis in the UK, which can be as large as  $M$  7.1 (e.g. Tromans et al. 2019; Mosca et al. 2022). Ground-motion samples were generated from  $M$  3.0 to  $M$  7.75, using a step of 0.25 magnitude units. Bommer et al. (2007) evidence edge effects at the limits of their empirical dataset; such statistical artefacts would occur even when using simulated data. Hence, we extend the simulations 0.5 magnitude units above and below the recommended magnitude range:  $M$  3.5 to 7.25, which is above any likely maximum magnitude within UK seismic hazard assessments.

Although earthquake ground motions from  $R_{JB} > 300$  km are unlikely to be of engineering interest, even for the largest earthquakes, ground-motion samples were generated from  $R_{JB} = 0$  km to  $R_{JB} = 1000$  km at 16 roughly logarithmically-spaced distances. The main reason for this is that there are instrumental and macroseismic data from UK-region earthquakes with  $M > 5$  from  $R_{JB} > 300$  km and so having a robust model that can be compared to these data is desirable as this critical magnitude range is sparsely sampled at closer distances. As the Chiou and Youngs (2014) GMPE is only recommended for use by its developers up to 300 km, the approach proposed by Campbell (2003) is used for greater distances. This approach consists of scaling the samples for  $R_{JB} > 300$  km by the factor needed to make the stochastic and HEM estimates match at  $R_{JB} = 300$  km. Campbell (2003) used 70 km for this critical distance because the older empirical models he used were not reliable at greater distances. The adoption of Chiou and Youngs (2014) for this study makes it possible to extend this critical distance to 300 km. For the convenience of future users, models for both  $R_{JB}$  and  $R_{RUP}$  have been derived (for the remainder of the article only the models using  $R_{JB}$  are discussed for simplicity—the models using  $R_{RUP}$  are almost identical except for  $R < 30$  km). It was checked that for mutually consistent scenarios, predictions from the two sets of models matched.

Finally, we also wished to provide a GMM that covers the spectral period range of interest to engineering applications. Therefore, spectral accelerations were generated for a closely-spaced set of 19 spectral periods from 0.01 s (assumed to be equal to peak ground acceleration, PGA) to 10 s. Coefficients are only provided for 5% damping, which is the standard choice for GMMs. If needed, damping scaling factors based on large datasets such as those by Rezaeian et al. (2014) or Akkar et al. (2014) may be applicable to adjust the predictions to other damping ratios.

Once the spectral acceleration samples for every magnitude, distance and spectral period were generated by CHEEP, a series of regression analyses were performed to develop a suite of 162 GMPEs for each combination of the stochastic parameters for the target (UK) region (see Sect. 3). The same functional form used by Campbell (2003), and Douglas et al. (2006) for southern Norway, was adopted but with a modification to the distances at which the geometric spreading rate changes to  $r_1 = 50$  km and  $r_2 = 100$  km (from 70 and 130 km):

$$\ln Y = c_1 + f_1(M) + f_2(M, R_{JB} \text{ or } R_{RUP}) + f_3(R_{JB} \text{ or } R_{RUP})$$

$$f_1(M) = c_2 M + c_3 (8.5 - M)^3$$

$$f_2(M, R) = c_4 \ln R + (c_5 + c_6 M)R$$

$$R = \sqrt{R_{JB} \text{ or } R_{RUP} + [c_7 \exp(c_8 M)]^2}$$

$$f_3(R_{JB} \text{ or } R_{RUP}) = 0 \quad \text{for } R_{JB} \leq r_1$$

$$f_3(R_{JB} \text{ or } R_{RUP}) = c_9 [\ln(R_{JB} \text{ or } R_{RUP}) - \ln r_1] \quad \text{for } r_1 < R_{JB} \text{ or } R_{RUP} \leq r_2$$

$$f_3(R_{JB} \text{ or } R_{RUP}) = c_9 [\ln(R_{JB} \text{ or } R_{RUP}) - \ln r_1] + c_{10} [\ln(R_{JB} \text{ or } R_{RUP}) - \ln r_2] \quad \text{for } R_{JB} \text{ or } R_{RUP} > r_2$$

It was confirmed (see Electronic Supplement) that this functional form closely matched the samples at all magnitudes and distances (including close to the edges of the magnitude-distance space). As discussed below, this suite of 162 GMPEs is cumbersome and time-consuming to use within most hazard assessments; therefore, a resampling approach was implemented to create a more usable GMM that retains the centre, body and range of the ground-motion distribution.

### 3 Stochastic models for the UK

In this section, following a summary of the collected instrumental data from the UK and surrounding areas, the stochastic models developed for the UK are described. These models are placed within a logic tree with initial weights assigned to the branches based on expert judgement. These weights were revised based on the fit with observations from the UK and surrounding region (northern France, Belgium, the Netherlands and northwestern Germany). The initial suite of potential models was developed using a literature review of previous stochastic models for the UK and surrounding region. The stochastic method has been used to predict ground motions for the UK since the pioneering work of Winter (1995). Key references for this review include Lubkowski et al. (2004), Edwards et al. (2008), Sargeant and Ottemöller (2009), Ottemöller and Sargeant (2010), Rietbrock et al. (2013) and Rietbrock and Edwards (2019). Based on this review, ranges for the key stochastic parameters were estimated using simplicity and physical arguments as well as considering potential trade-offs between parameters. The development of an early version of this suite of stochastic models was discussed by Douglas et al. (2023), who included various figures illustrating the choices that are not repeated here. Minor revisions to this suite have been made since the conference article was written. Standard choices are assumed for the other input parameters to the stochastic method (e.g., radiation pattern factor); changing these fixed parameters within the range of possible values has a negligible impact on the predicted ground motions (see the Electronic Supplement for a summary of these).

#### 3.1 Database of ground motions from the UK and surrounding region

A database of ground-motion records, and macroseismic data (i.e., intensity data points, IDPs), from the UK [from the British Geological Survey, (BGS 2022a,b)] and surrounding

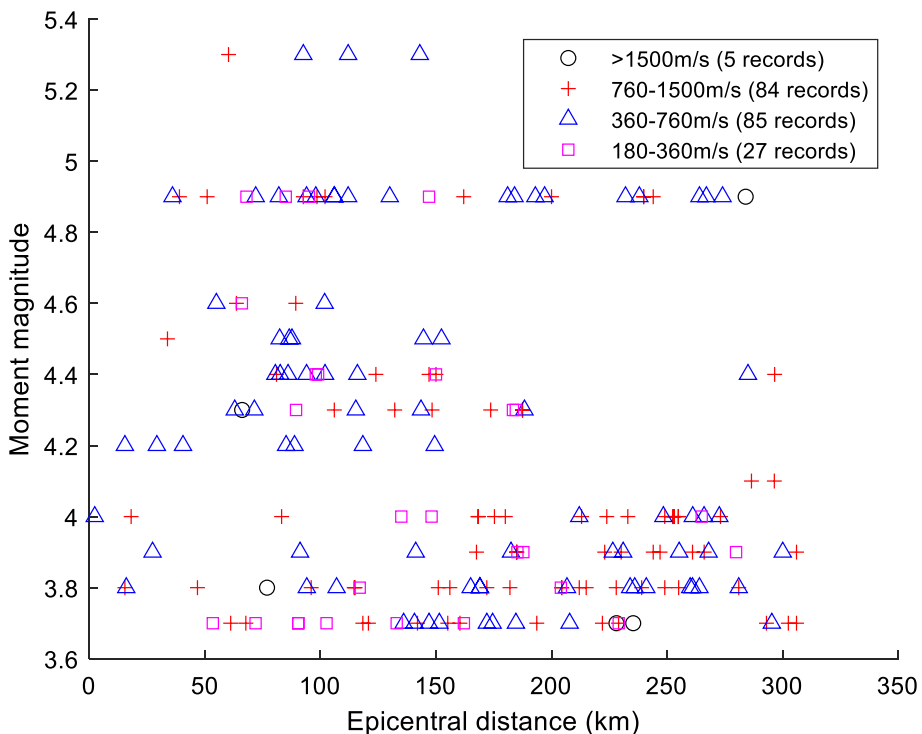


**Fig. 1** Magnitude-distance-site class distribution of data in the database from the UK and surrounding region

region [France (RESIF 1995a,b, 2022; BCSF 2022; BRGM et al. 2022) and Belgium (ROB 2022)] was compiled and processed to obtain parameters of engineering interest (here pseudo-spectral accelerations, PSAs, at various structural periods), by Jacobs in recent UK nuclear-related projects. The database contains records from notable UK earthquakes (1999 to 2020) such as Folkestone 2007 (**M** 4.0), Market Rasen 2008 (**M** 4.9) and Swansea 2018 (**M** 4.3), and data from significant earthquakes in adjacent regions (1992 to 2019) such as St Die (France) 2003 (**M** 4.9) and Roermond (The Netherlands) 1992 (**M** 5.3).

This database consists of 201 three-component records, from a mixture of strong-motion, broadband and short-period instruments, of 26 events with **M** between 3.7 and 5.3 and  $R_{\text{epi}} < 300$  km, with most of the data being from  $R_{\text{epi}} > 50$  km (Fig. 1). The database also includes 18,610 IDPs, for intensity III and higher, from 31 events from the UK and surrounding region with **M** between 3.7 and 5.4 and  $R_{\text{epi}} < 300$  km. Even though our model is derived for source-to-site distances up to 1000 km, we do not consider instrumental data from beyond 300 km because of low signal-to-noise ratios of these records.

Due to the relatively small database, the lack of data from larger magnitudes and closer distances and the limited local site information, the inversion of these data to determine the parameters of stochastic models is highly nonunique. The time-averaged shear-wave velocities in the top 30 m ( $V_{S30}$ ) for all stations in this database were estimated using available information (e.g., Tallett-Williams 2017; Villani et al. 2019), which is often quite limited, from a few dozen estimated (using various techniques) shear-wave velocity profiles, lithology from local boreholes in the BGS database, horizontal-to-vertical ratios and

an attempt at generalised inversion. These estimates were subsequently used to adjust the Fourier amplitudes of the ground-motion records to a uniform reference of  $V_{S30}=900$  m/s (see Sect. 3.7) using the site-amplification terms of the GMM of Bayless and Abrahamson (2019). This adjustment approximately removes the site amplification coming from velocity impedance contrasts, but not site-specific effects due to resonance. Because the  $V_{S30}$  of most sites (81% of records) is  $>500$  m/s and the mean  $V_{S30}$  of all records is 699 m/s, the effect of the site adjustment is moderate. The site-adjusted ground-motion records are used to reweight the branches of the GMMs and to compare them with predictions from the GMM.

### 3.2 Depth to top of rupture

The Chiou and Youngs (2014) GMM used for the host region includes a term to model the effect of the depth to the top of rupture ( $Z_{TOR}$ ). Therefore, if  $Z_{TOR}$  is not characterised for the target region (here, the UK) then we are making the implicit assumption that the average  $Z_{TOR}$  is comparable in the two regions. Given the deeper seismogenic layer in the UK (25 km to 30 km) (e.g. Rietbrock et al. 2013) than in coastal California (15 km to 20 km) (e.g. Zeng et al. 2022), where most of the data used to create the Chiou and Youngs (2014) model are from, it is unlikely that this assumption is valid. The  $Z_{TOR}$  model has a considerable impact in the near-source region ( $R_{JB} < 20$  km), but its impact becomes negligible at  $R_{JB} > 50$  km as the horizontal distance from the source dominates over the effect of depth. As the largest UK earthquakes with instrumental depths are around **M** 5.0 and macroseismic depths for larger events are poorly constrained, there is uncertainty in this parameter for the UK. The approach followed to develop models for  $Z_{TOR}$  is discussed in this section.

Recent seismic hazard assessments for sites in the UK (Tromans et al. 2019; Villani et al. 2020; Mosca et al. 2022) and surrounding countries (e.g., Grünthal et al. 2018; Drouet et al. 2020; Martin et al. 2018) characterise the focal depth distribution of their source zones, but these characterisations are generally magnitude independent and based mainly on instrumentally-determined focal depths, which are generally from **M** < 5.5. Therefore, the focal depths from three catalogues: BGS's instrumental catalogue (from 1970),<sup>3</sup> BGS's Significant British Earthquakes (up to 1970)<sup>4</sup> and a French catalogue FCAT-17 (Manchuel et al. 2018) were used as a basis for the development of the  $Z_{TOR}$  models for this study. The rupture width was predicted from the published **M** estimates using the equations of Leonard (2014).<sup>5</sup> Combining this rupture width with the published focal depth assuming that the focal depth is 60% down the rupture width (Mai et al. 2005), which is the assumption made by Kaklamanos et al. (2011), and assuming vertical strike-slip ruptures, leads to an estimate of the  $Z_{TOR}$  for each earthquake. A graph showing **M** against estimated  $Z_{TOR}$  is shown in Fig. 2. Also included on this plot is the mean depth from binning the instrumental depth estimates from both BGS and FCAT-17 into 0.2 M unit intervals. FCAT-17 includes dip-slip rupture events, which means some  $Z_{TOR}$  values are underestimated. However, given the already large uncertainties in these estimates and because we do not use these  $Z_{TOR}$  values directly, we believe that the assumption of vertical ruptures is acceptable. Trial focal depths of 5 km, 10 km, 15 km and 20 km used by the BGS and other seismological agencies when

<sup>3</sup> <http://earthquakes.bgs.ac.uk/earthquakes/dataSearch.html>

<sup>4</sup> <http://www.earthquakes.bgs.ac.uk/earthquakes/UKsignificant/index.html>

<sup>5</sup> Using the equations of Wells and Coppersmith (1994) leads to similar conclusions.

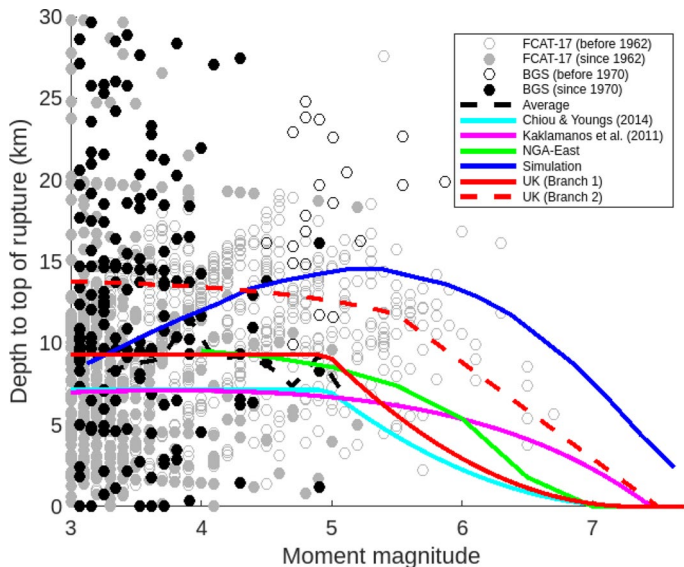


**Fig. 2** Estimated depths to top of rupture for earthquakes in the FCAT-17 and BGS databases (separated into pre-instrumental and instrumental periods), their binned averages, and four candidate models for average  $Z_{\text{TOR}}$  with magnitude and the two developed  $Z_{\text{TOR}}$  models. "Simulation" refers to the exercise discussed in the text where ruptures with widths based on observed UK focal depths are simulated and average  $Z_{\text{TOR}}$  values estimated

locating earthquakes are noticeable in Fig. 2 as lines of points centred around these values. This indicates significant uncertainties associated with these values.

On Fig. 2 three published models for  $Z_{\text{TOR}}$  are plotted: the model of Chiou and Youngs (2014) based on published  $Z_{\text{TOR}}$  estimates for the largest earthquakes in their database; a model developed by Kaklamanos et al. (2011) from the same database; and a model for Central and Eastern North America (CENA) that was developed as part of the NGA-East project (PEER 2015). The  $Z_{\text{TOR}}$  estimates from the UK and surrounding area are on average deeper than those from these other models, particularly those of Chiou and Youngs (2014) and Kaklamanos et al. (2011). Additionally, the  $Z_{\text{TOR}}$  estimates from events occurring before 1970 (and hence with focal depths mainly estimated from macroseismic data) suggest a slight positive magnitude dependence (i.e. larger earthquakes have larger  $Z_{\text{TOR}}$ ). This positive magnitude dependency has been noted before (e.g. Ambraseys and Jackson 1985; Main et al. 1999); however, for the largest earthquakes ( $M > 6.0$ ) extrapolation of this trend would be difficult to justify given the lower depth limit imposed by the thickness of the seismogenic layer (25–30 km).

To understand this apparent contradiction the following simulations were conducted. For simplicity, vertical strike-slip faulting earthquakes were assumed because, as noted previously, Baptie (2010) showed that most focal mechanisms computed for UK earthquakes indicate strike-slip faulting. In the simulation exercise, a linear regression equation was first fitted to the focal depths in the BGS's Significant British Earthquakes list (this excludes the large number of events with  $M < 3.7$ ). Next, a random magnitude taken from a uniform distribution between  $M$  3.0 and  $M$  7.75 was generated and a focal depth estimated using this regression equation (and its homoscedastic standard deviation), assuming that it can be extrapolated to magnitudes beyond the observations, which end at  $M$  5.9. Then,

$Z_{\text{TOR}}$  and  $Z_{\text{BOR}}$  (depth to the bottom of the rupture) were estimated from this focal depth in the same way as for the actual earthquakes listed in the BGS catalogues and FCAT-17. If  $Z_{\text{TOR}}$  was less than 0 km (i.e. surface rupture) or  $Z_{\text{BOR}}$  was greater than 25 km (i.e. seismogenic thickness), then the process was repeated until physically acceptable depths were obtained. This simulation exercise (repeated 50,000 times) showed that the observed magnitude-dependency of focal depths is compatible with a  $Z_{\text{TOR}}$  model that approaches zero for  $M > 7.0$ . This occurs because focal depths approach an asymptote around 20 km from around  $M 5.5$  as they cannot get deeper and still fit an increasingly wide rupture within the seismogenic layer. Given the uncertainties in the focal depths derived from macroseismic intensities and the lack of similar strong magnitude dependency in other parts of the world, we did not think it justifiable to use the results from the simulations to create a  $Z_{\text{TOR}}$  model.

Based on the observations in Fig. 2 and the simulation exercise, two models for  $Z_{\text{TOR}}$  are used as separate branches in the logic tree. The first equation (assigned a weight of 60%) is the one of Chiou and Youngs (2014) multiplied by a factor of 1.3 to better match the mean  $Z_{\text{TOR}}$  estimates from the FCAT-17 and BGS catalogues for  $M < 5.0$  and the fact that the seismogenic layer in the UK is considerably thicker than that in California. The second model (assigned a weight of 40%) is bilinear and comprises a  $Z_{\text{TOR}}$  line up to  $M 5.5$  that is equal to the weighted mean of the focal depths in the UK National Seismic Hazard Model (Mosca et al. 2022) of 14 km minus 60% of the rupture width estimated by the equations of Leonard (2014), and then, a straight line from 11.8 km (the value at  $M 5.5$  from the first line) to 0 km at  $M 7.5$ . These two models are indicated in Fig. 2. Using these two  $Z_{\text{TOR}}$  models will increase epistemic uncertainty in the predicted near-source ground motions, which we consider appropriate given the sparse observations from  $R_{\text{epi}} < 50$  km.

### 3.3 Source spectral shape

Edwards et al. (2008) found that the single-corner  $\omega^2$  Brune (1970, 1971) spectral shape clearly fits the observed spectra from 33 near-source records of UK earthquakes with local magnitudes ( $M_L$ ) between 2.0 and 3.0 better than two other single-corner spectral shapes, namely  $\omega^3$  and Boatwright (1978). Almost all UK studies use this classic spectral shape. Double-corner spectral shapes (e.g., Joyner 1984) imply a breakdown in the 1:1 scaling relation between seismic moment and fault dimensions (i.e., a fault aspect ratio no longer equal to 1.0). This additional complexity is not needed for this study given the relatively small earthquakes that occur in the UK, its relatively thick seismogenic layer (25 to 30 km) and the use of the HEM, which corrects the long-period spectral shape using an empirical model. Hence, we adopt the single-corner  $\omega^2$  Brune (1970, 1971) shape for our stochastic models. This decision is revisited below.

### 3.4 Geometric spreading

Many geometric spreading (decay) models for the UK include a  $1/R$  branch (spherical spreading) for near-source distances and a  $1/\sqrt{R}$  branch (cylindrical spreading) for far-source distances (e.g., Lubkowski et al. 2004). Several models also include a middle branch with little or no decay to model the arrival of critical reflections off the Mohorovičić discontinuity (Moho). The distances at which the transitions between the different branches occur vary amongst the models.

The depth of the Moho below the UK is  $33 \pm 5$  km according to the global crustal structure model CRUST1.0 (Laske et al. 2013). Using this information, the ratio of the

shear-wave velocities above and below the Moho (about 0.8), the probable focal depths for UK earthquakes (between 5 and 25 km) and Snell's law, reflections off the Moho would occur between about 40 and 75 km. This confirms the use of 50 km for the start of this flat branch proposed by Edwards et al. (2008), Rietbrock et al. (2013) and Rietbrock and Edwards (2019). Several UK models (e.g. Sargeant and Ottemöller 2009; Rietbrock and Edwards 2019) use 100 km as the start of the cylindrical spreading branch.

Based on this information the following three branches and *a priori* weights [within square brackets] are proposed:

- $1/R$  to 100 km and then  $1/\sqrt{R}$  for greater distances—[0.25]
- $1/R$  to 50 km, no decay until 100 km then  $1/\sqrt{R}$  for greater distances—[0.50]
- $1/R$  to 75 km and then  $1/\sqrt{R}$  for greater distances—[0.25]

The branch with a flat (no decay) portion between 50 and 100 km is given the highest weight because Moho “bounce” effects are common in GMMs for SCRs [e.g. the CENA GMMs of EPRI (2004)] and previous detailed analysis of UK data (Edwards et al. 2008; Rietbrock et al. 2013; Rietbrock and Edwards 2019) provide strong evidence for such effects.

### 3.5 Path attenuation

Three main models for UK anelastic attenuation ( $Q$ ) have been proposed in the literature. Based on previous analyses that showed a close match with observations, we adopt the Sargeant and Ottemöller (2009) relationship,  $Q = 266 f^{0.53}$  as our central model. This model is simpler than those of Edwards et al. (2008) and Rietbrock and Edwards (2019), who proposed depth-dependent but frequency-independent models. The model of Sargeant and Ottemöller (2009) is also easier to implement within SMSIM than the other two candidate models.

Sargeant and Ottemöller (2009) identify regional dependency in  $Q$  within the UK (their Fig. 8). The minimum and maximum values of  $1/Q_{Lg}$ , i.e. the inverse of the value of  $Q$  for Lg waves (multiple-reflected shear waves), shown in Fig. 8 of Sargeant and Ottemöller (2009), are used to construct two alternative models to capture the regional variations in  $Q$  and epistemic uncertainty. Based on these values, lower and upper  $Q$  models were estimated by eye to capture the observed trend in these minimum and maximum estimates: 230  $f^{0.5}$  (lower) and 330  $f^{0.6}$  (upper). These  $Q$  models are similar to models for the UK (Rietbrock and Edwards 2019), France (Campillo and Plantet 1991) and southern Netherlands (Goutbeek et al. 2004). Attenuation in the UK is clearly higher (lower  $Q$ ) than in Scandinavia (e.g. Kvamme et al. 1995). The central branch is assigned an *a priori* weight of 0.630 and the lower and upper branches weights of 0.185. These weights correspond to the 50th (median), 5th and 95th percentiles, respectively, in the three-point approximation for continuous random variables proposed by Keefer and Bodily (1983). As shown by Scherbaum et al. (2005, their Fig. 10) the impact of uncertainty in  $Q$  on ground-motion uncertainty is small, particularly for  $R_{epi} < 50$  km, which is the most important distance range for UK seismic hazard. Because, however, earthquakes at greater distances can be important for some locations [e.g. see disaggregation for Edinburgh provided by Mosca et al. (2022), their Fig. 17] it was considered important to capture uncertainty in this input parameter.

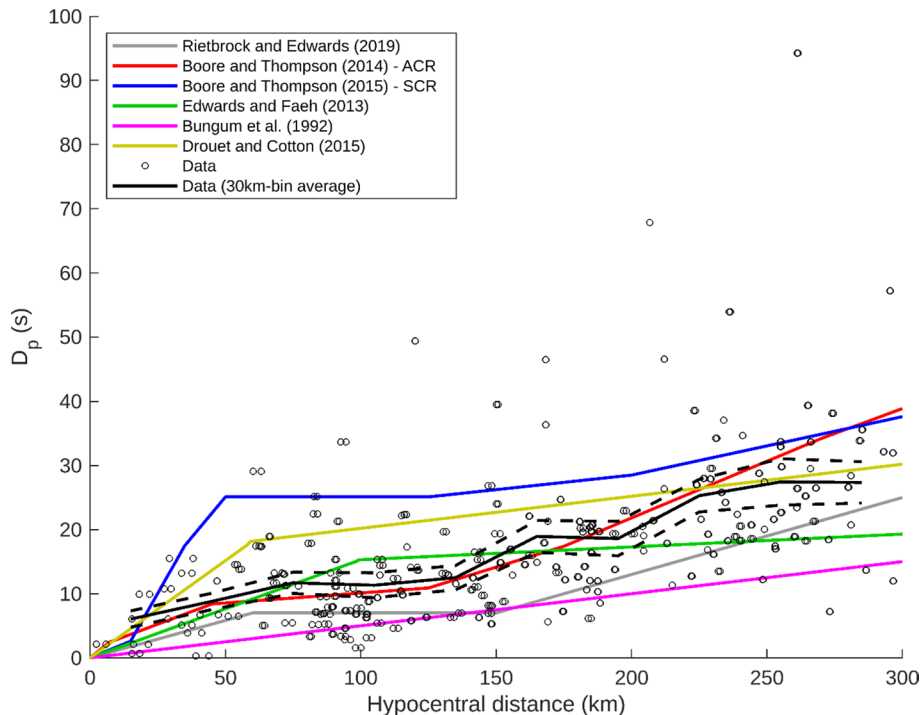


**Fig. 3** Candidate path duration models and observed path durations from the ground-motion database with the means (and 95% confidence intervals) averaged within 30 km intervals. The model of Boore and Thompson (2014)—ACR was chosen for the final logic tree

### 3.6 Path duration

Path duration refers to how seismic waves spread out in the time domain as they propagate from the earthquake source. Rietbrock et al. (2013) and Rietbrock and Edwards (2019) propose a path duration model for the UK. Boore and Thompson (2014) provide a model for ACRs. This model is repeated in Boore and Thompson (2015), who also provide a model for SCRs. Other proposed path duration models relevant for this study include those of Edwards and Fäh (2013) for Switzerland, Bungum et al. (1992) for Norway and the surrounding region, and Drouet and Cotton (2015) for the French Alps.

To assess the applicability of these models, durations are examined from the collected instrumental data using Husid plots and the approach of Boore and Thompson (2014), which consists of examining the duration estimated by  $D_{95} = 2(D_{80} - D_{20})$ , where  $D_{95}$  is the time between the 5th and 95th percentiles of the Arias intensity,  $D_{80}$  is the time to the 80th percentile and  $D_{20}$  is the time to the 20th percentile. The estimated source durations [using Eq. 6 of Atkinson and Silva (2000) as also used by Boore and Thompson (2014)] for each record are subtracted from these observed durations and these estimated path durations ( $D_p$ ) are plotted alongside the candidate path duration models (Fig. 3). To compare the estimated path durations with the candidate models, the arithmetic means (and their 95% confidence intervals) within 30 km width bins (e.g. 0–30 km and 30–60 km) are plotted on the figure. The path duration model for ACRs proposed by Boore and Thompson (2014)

best matches the means in each bin for all distances, although it is potentially slightly over-predicting the observed durations beyond about 250 km. Therefore, this model is adopted for the path duration component. This is also the path duration model used by Stafford et al. (2022) for the host stochastic model. Aldama-Bustos and Strasser (2019) examine the strong-motion durations of UK and find that a duration model derived mainly from Californian data (Bommer et al. 2009) is the best fitting model to the observations. Due to its limited impact on predicted spectral accelerations [e.g. Fig. 10 of Scherbaum et al. (2005)] and the close match between the observations and model (Fig. 3) no uncertainty in this parameter is included within the logic tree.

### 3.7 Site amplification

There is considerable spatial variation in shear-wave velocity ( $V_S$ ) profiles (even within a relatively small country such as the UK) as well as epistemic uncertainty due to the limited number of measured profiles. Rather than using different  $V_S$  profiles to capture the variation and uncertainty, we assume a single  $V_S$  profile representative of a generic site with out-cropping chalk in southern England. Based on experience from various site-specific hazard studies (Tromans et al. 2019; Aldama-Bustos et al. 2023), we believe that the adopted profile is generally applicable to weak rock sites in the UK. Hard rock sites that occur in northern England, much of Scotland and Wales are excluded. Adjustments of the model to other site conditions could be undertaken using the reported  $V_S$  profile and a  $V_S$ -kappa adjustment (e.g., Al Atik et al. 2014), or by updating the stochastic model with this new  $V_S$  profile (and potentially other kappa values) and then using this within the HEM.

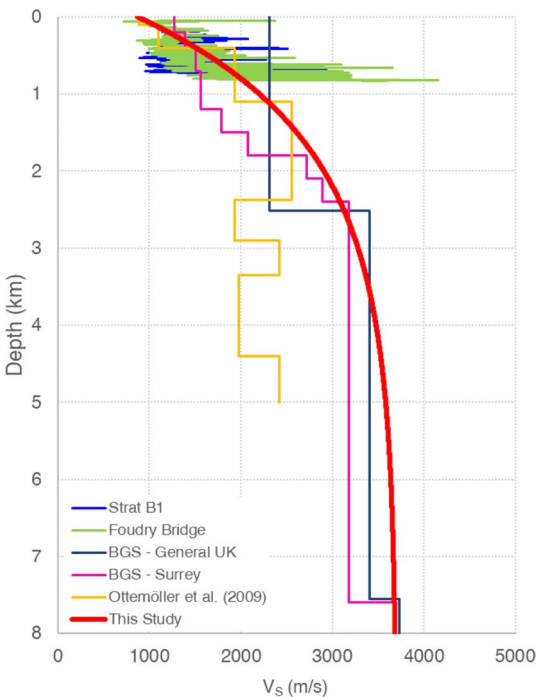
Several  $V_S$  profiles for UK sites, particularly those with reasonable resolution in the upper 2 km, from the literature were examined. These include profiles used by the BGS for locating earthquakes [BGS—General UK (Turbitt 1984) and BGS—Surrey (Galloway 2021)], profiles reported in articles on specific earthquake sequences (Ottemöller et al. 2009), and oil-prospecting profiles in the Berkshire region that are in the public domain (Strat 1 and Foudry Bridge boreholes). These profiles along with the  $V_S$  profile considered in this study are presented in Fig. 4.

We used the functional form of the Poggi et al. (2011) profile to parameterise the  $V_S$  profile (Eq. 1, where  $z$  is the depth from the surface). The coefficients in the Poggi et al. (2011) function were varied to find the best visual fit to the available profiles. The final coefficients chosen were:  $b_1 = 1.1$ ,  $b_2 = 150$ ,  $V_{S\min} = 873$  m/s and  $V_{S\max} = 3700$  m/s, which correspond to the  $V_S$  at the surface and at around 10 km. The  $V_{S30}$  of the final profile is 900 m/s, placing the profile well inside Site Class A (rock), corresponding to  $V_{S30} \geq 800$  m/s, of Eurocode 8, which applies in the UK (e.g. Mosca et al. 2022).

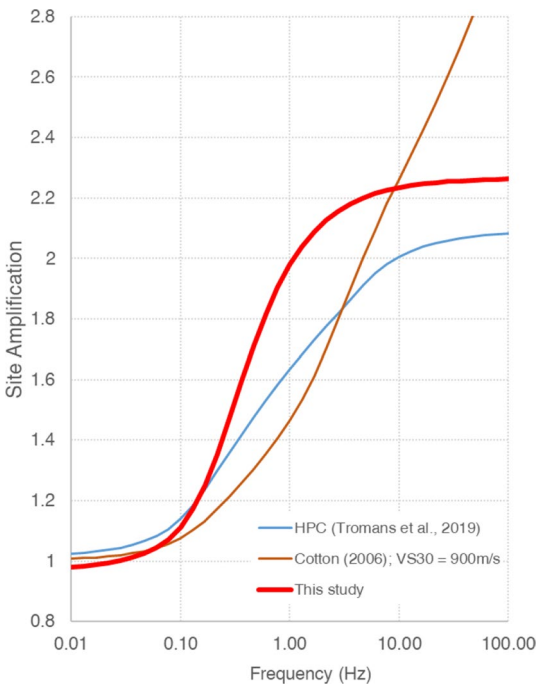
$$V_S(z) = (V_{S\max} - V_{S\min}) \left[ 1 - b_1^{-z/b_2} \right] + V_{S\min} \quad (1)$$

Site amplification from the quarter-wavelength method depends on the  $V_S$  profile as well as the density profile. For this study the  $V_S$ -density correlation proposed by Boore (2016) is adopted to estimate density for all depths based on the  $V_S$  computed from Eq. 1. Available data from a representative range of UK geological units (Lias and Mercia Mudstone Groups from southwestern England, Sherwood Sandstone Group from northern England, and the Thames, Lambeth and Chalk Groups from eastern England) were used to confirm that this relationship is appropriate for the UK. The site amplification corresponding to the  $V_S$  profile considered in this study is presented in Fig. 5. For comparison Fig. 5 also

**Fig. 4** Comparison of publicly available  $V_S$  profiles for southern England with the target  $V_S$  profile for this study



**Fig. 5** Site amplification for the target  $V_S$  profile for this study. For comparison, the site amplification corresponding to the  $V_S$  profile used by Tromans et al. (2019) for the HPC PSHA, and the Cotton et al. (2006) profile obtained for a  $V_{S30}$  of 900 m/s, are also presented



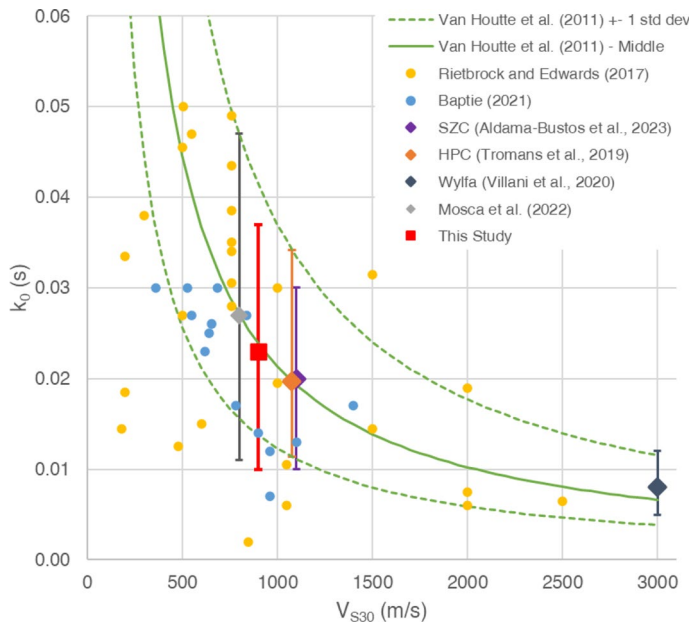


**Fig. 6** Summary of  $\kappa_0$  estimates available for the UK and the  $\kappa_0$  model proposed in this study

presents the site amplifications for the  $V_s$  profile considered by Tromans et al. (2019) for the Hinkley Point C (HPC) PSHA, with a  $V_{S30}$  of 1000 m/s, and the  $V_s$  profile from Cotton et al. (2006) for a  $V_{S30}$  of 900 m/s.

### 3.8 Site attenuation

We model site attenuation using the standard approach of a kappa filter (Anderson and Hough 1984) and assume that the Q model accounts for path attenuation. We define a range of  $\kappa_0$  (kappa at  $R_{epi}=0$  km) values appropriate for the (generic rock)  $V_s$  profile. Rietbrock and Edwards (2017) and Baptie (2021) provide  $\kappa_0$  estimates for various BGS stations. Mosca et al. (2022) considered the  $\kappa_0$  estimates from Baptie (2021) to define the  $\kappa_0$  logic tree used for the development of the UK national seismic hazard maps. Additionally, Villani et al. (2020), Tromans et al. (2019) and Aldama-Bustos et al. (2023) provide  $\kappa_0$  estimates, along with their uncertainty ranges, for the Wylfa Newydd, Hinkley Point C (HPC) and Sizewell C (SZC) sites respectively. Also, we undertook various analyses of the ground-motion data using the approach of Anderson and Hough (1984).

Based on these studies and considering a  $V_{S30}$  of 900 m/s (i.e., the  $V_{S30}$  of the selected  $V_s$  profile), three alternative  $\kappa_0$  values are proposed: 0.010 s, 0.023 s and 0.037 s, as the upper, central (i.e., best estimate) and lower estimates with *a priori* weights of 0.185, 0.630 and 0.185. Figure 6 presents a comparison of the  $\kappa_0$  values from the studies mentioned above with the  $\kappa_0$  branches proposed in this study. Also shown in Fig. 6 are  $\kappa_0$  estimates, and associated uncertainty, predicted by the  $\kappa_0$ - $V_{S30}$  relationship of Van Houtte et al. (2011), which has been used in several recent studies to assess  $\kappa_0$ . The proposed  $\kappa_0$  model is in good agreement with estimates for UK national hazard maps, HPC and SZC, which

correspond to  $V_{S30}$  values relatively close to the one proposed for the current study. In the case of SZC, it also corresponds to similar geological conditions (i.e., weak rock).

### 3.9 Stress drop

Due to the uncertainty surrounding how stress drop (also called stress parameter) scales with magnitude and potential trade-offs with other stochastic parameters, we estimate appropriate values for larger earthquakes ( $M > 5.5$ ) (for which UK data are not available but which are important for hazard assessments) using the approach discussed below. For smaller earthquakes, the residuals from the resulting GMMs for the observed ground motions are subsequently used to assess whether these values need modifications for  $M < 5.5$  (as shown in Sect. 4.2 the values did not need updating). As earthquakes with magnitudes higher than have been instrumentally observed are the most important for engineering purposes, we considered this approach appropriate because the extrapolation from stress drops of smaller events is highly uncertain.

A preliminary assessment of stress drop from the instrumental data showed little magnitude dependency and an overall best single stress drop of 100 bars (10 MPa) (Douglas et al. 2023). This result was stable using different spectral period ranges (0 to 1 s or up to 5 s) and geometric spreading rates (central or upper branches). This high stress drop and little magnitude dependency contrasts with the behaviour evidenced in Fig. 2 of Rietbrock et al. (2013), with lower values and a clear magnitude dependence. To capture this, Rietbrock et al. (2013) developed two models: a) a self-similar (magnitude-independent) model where the median stress drop is 18 bars (1.8 MPa) for all magnitudes, and b) a magnitude-dependent model where the median stress drop is 7 bars (0.7 MPa) for  $M \leq 3$  and increases linearly to 100 bars (10 MPa) at  $M = 4.5$  and then stays constant for larger magnitudes. Therefore, the lack of magnitude dependency of the inverted stress drops was quite surprising. This could be because of the choice of the other stochastic parameters, in particular the site attenuation ( $\kappa$ ), and the associated strong trade-offs.

To choose the branches of the stress drop, an approach like that used by Bommer et al. (2022) for the Groningen (The Netherlands) gas field was applied. In this approach, predictions from empirical GMMs from other regions for  $M = 5.5, 6.0$  and  $6.5$  and a near-source distance ( $R_{JB} = 20$  km), where the empirical models are well constrained and differences due to path attenuation are small, are compared to predictions from the suite of predictions from the UK hybrid model for a range of stress drops from 20 to 200 bars (in steps of 20 bars). This approach assumes that average near-source ground motions from moderate and large earthquakes in the UK are similar to those in other regions, which are not necessarily tectonically analogous. Any estimate of the stress drop for UK events with  $M > 5.5$  would be an assumption given the complete lack of near-source data for this magnitude range. We believe that the assumption that near-source UK ground motions are similar to better observed regions is the most defensible. The weighted mean of the predictions from the hybrid model are used, although because of the short source-to-site distance chosen, only variations in  $\kappa$  have a strong impact on the predictions. The GMPEs used by Aldama-Bustos et al. (2023) within their GMM for the SZC site, excluding the Rietbrock and Edwards (2019) model because it is not constrained at large magnitudes, were adopted as appropriate choices for this analysis. Constant values of the stress drop needed to obtain the best match between these ground-motion predictions are subsequently chosen.

Figure 7 shows the results of this analysis for  $M = 6.0$  (the comparisons for  $M = 5.5$  and  $M = 6.5$  are very similar). This comparison shows that using a value of 20 bars leads to

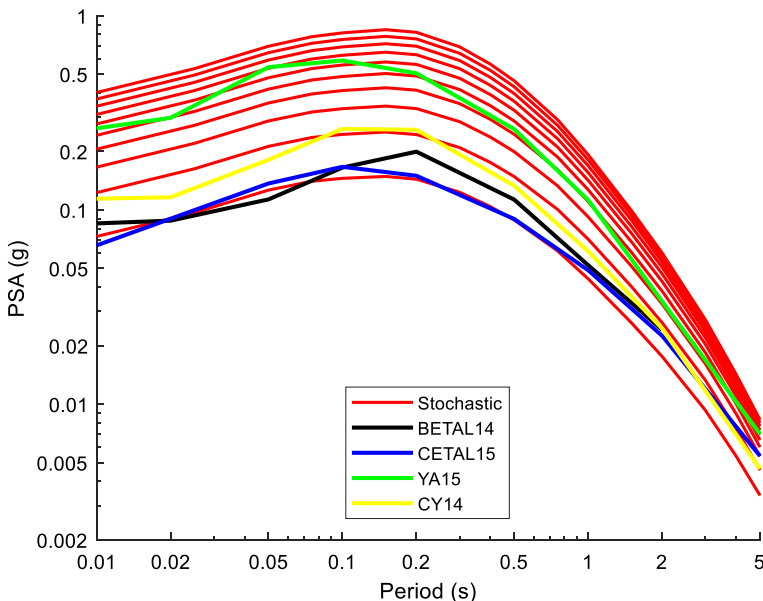


**Fig. 7** Comparison of predictions for a M 6.0 earthquake at 20 km from four empirical GMPEs and predictions from the *a priori* weighted mean of the UK hybrid model with stress drops equal to 20 to 200 bars in steps of 20 bars (red lines). BETAL14 is Bindi et al. (2014), CETAL15 is Cauzzi et al. (2015), YA15 is Yenier and Atkinson (2015) and CY14 is Chiou and Youngs (2014)

a close match to the lowest predictions from the empirical GMPEs [either Cauzzi et al. (2015) or Bindi et al. (2014)] and 140 bars leads to a match to the predictions from the GMPE predicting the highest spectrum (Yenier and Atkinson 2015) with 80 bars providing a prediction roughly in the middle. Based on this comparison three stress drops (i.e., 20, 80 and 140 bars) are used to develop the final model with *a priori* weights of 0.185, 0.630 and 0.185, respectively.

It is worth mentioning that the response spectral shape from the stochastic (rather than the hybrid) model is slightly flatter than the shape from the empirical models, which means that choosing a stress drop that is appropriate for  $T < 1$  s leads to over-predicting spectral accelerations for  $T > 1$  s. The HEM, through the use of the ratio of stochastic models (both of which here assume single-corner spectral shapes) and the empirical host model (Chiou and Youngs 2014), corrects for this mismatch in the long period spectral shape. Therefore, it is not necessary to modify the stochastic models (e.g., using a double-corner spectral shape) to address this mismatch. This is an advantage of the HEM over using the target stochastic models directly.

Additionally, because the match between the host empirical and stochastic models is close (particularly for  $T < 1$  s) due to the care that Stafford et al. (2022) took in developing the stochastic model, predictions from the hybrid models generally closely match predictions from the UK stochastic models. The exception to this is for  $T > 1$  s and larger earthquakes ( $M > 6$ ) where the adoption of the single-corner spectral shape leads to significant differences. This means that if a different host empirical model was used within the HEM the resulting hybrid models would be similar, as long as a well-matched associated stochastic model was used.

## 4 Comparison of predictions from the model to observations

In this section the GMMs developed are compared with the instrumental data from the UK and surrounding region to adjust the *a priori* branch weights so that the complete model shows limited bias. The 162 branches are then resampled using both the *a priori* and adjusted weights to obtain three- and five-branch versions that are easier to use in applications. A residual analysis shows that the weighted mean estimates from these resampled models are unbiased with respect to magnitude, distance and focal depth. Finally, comparisons with other instrumental and macroseismic data, which were not used for the derivation of the model, are presented.

### 4.1 Reweighting of the logic-tree branches using instrumental data

The logic-tree branches and weights defined in Sect. 3 were based on prior knowledge for the UK and were not directly based on instrumental or macroseismic data. Therefore, these observations can be used to update the default weights to reflect this additional information using a Bayesian approach. The log-likelihood approach of Scherbaum et al. (2009) and the ground-motion database described in Sect. 3.1 is used to update the original weights of the 81 branches for the  $Z_{\text{TOR}}$  variant with the highest weight (branch 1). This approach was also used by Douglas (2018) when he reweighted his backbone models for Europe and the Middle East for trial applications in specific regions.

The total residuals computed using the site-adjusted instrumental data collected from the UK and surrounding region were used within the equations provided by Scherbaum et al. (2009) in terms of log-likelihoods. For consistency with the origin of the 81 branches (from a set of stochastic models that can be used to generate ground motions for all spectral periods) updated weights are applied to all spectral periods together (i.e. weights do not vary with period). Five periods (0.01, 0.1, 0.2, 0.5 and 1.0 s) were used to estimate these updated weights to avoid overemphasising the short spectral periods within the calculations. Response spectral periods greater than 1.0 s were not used for the reweighting because of low-frequency noise in the ground-motion records, particularly those from small events at great distances. The differences between the updated weights for the two  $Z_{\text{TOR}}$  variants were negligible; hence, for simplicity, the same set of updated weights is proposed for both variants. To test the impact of the site adjustment, the revised weights were recomputed using the original data (i.e. with no adjustment to a common  $V_{S30}$  of 900 m/s) and the impact on the weights was less than 10% for all branches and less than 5% for all branches weighted at 1.5% or more in the final logic tree. This negligible impact of the site adjustment on the GMM is explained by 81% of data coming from sites with  $V_{S30} > 500$  m/s.

The impact of the weighting on the predictions from the model is minor within the first 70 km due to the sparsity of data at that distance. Beyond 70 km, the reweighting increases the prominence of the Moho “bounce” (the flat decay portion), which leads to higher predicted ground motions and narrows the spread between the 5th and 95th percentiles. Figure 8 shows plots of the mean bias based on total residuals for each of the 81 branches of the first  $Z_{\text{TOR}}$  variant against period as well as the original and adjusted weights for each branch. The figure shows that the low stress drop branches generally underestimate the observations (positive residuals) whereas the middle and higher stress drop branches show better agreement with the data. It also shows that the variation from the geometric



**Fig. 8** Mean bias based on total residuals (red dots, in terms of natural logarithms) against spectral period for each of the 81 branches. The branch numbers are indicated in the bottom-left corner of each graph as A-B-C-D, where A is the branch for the stress drop (left-to-right), B is the branch for the geometric spreading (top-to-bottom), C is the branch for Q (top-to-bottom within each  $3 \times 3$  square) and D is the branch for kappa (left-to-right within each  $3 \times 3$  square). The original and updated weights (expressed as a percentage) for each branch are indicated in the bottom-right corner of each graph

spreading branches is quite limited whereas the effect of kappa and, to a lesser extent Q, is more pronounced. Plots of the standard deviations of the total residuals (see Electronic Supplement) are similar for each branch and show standard deviations (in natural logarithms) of around 0.9 at 0.01 s, increasing to around 1.0 at about 0.2 s and then decreasing to around 0.8 at 2 s.

#### **4.2 Resampling to obtain an easier-to-use model**

The equations for the 162 branches (81 branches from the stochastic models for both  $Z_{\text{TOR}}$  branches) could be used within a seismic hazard assessment as the GMM. The impact of uncertainties in each component of the model could then be assessed and efforts could be made to reduce these uncertainties and revise the weights assigned to the corresponding branches. For example, if better information on the site attenuation ( $\kappa$ ) was available for a particular site then the weights of the three  $\kappa$  branches could be altered to reflect this improved knowledge.

This parameterisation of the GMM, although useful in a research context and potentially for some site-specific studies, would likely be too time-consuming to implement and run within most hazard assessments because of the large number of branches. Therefore, predictions from the GMM were resampled to provide an easier-to-use parameterisation of the model. To develop this parameterisation for each of the 19 spectral periods, the weighted distribution of the median ground motion estimates from the 162 logic-tree branches at each magnitude-distance point was sampled to find various

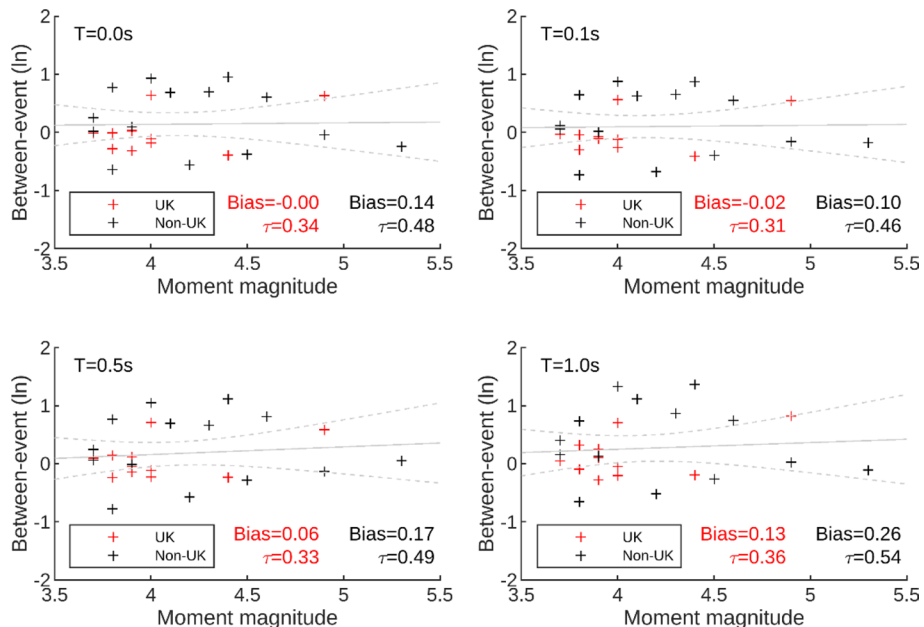


**Fig. 9** Between-event residuals, separated into events located in the UK (red symbols and text) and those located in the wider region (black symbols and text is when considering all events), against magnitude for the weighted mean of the three-branch parameterisation of the model. Grey lines are the linear best-fit line and its 95% confidence limits

percentiles. Firstly, the 5th, 50th (median) and 95th percentiles for the simplest (three-branch) parameterisation, using the respective weights of 0.185, 0.630 and 0.185 (Keefer and Bodily 1983), were computed. For a smoother parameterisation, the values at the cumulative probabilities of 0.035, 0.212, 0.500, 0.788 and 0.965 with weights of 0.101, 0.244, 0.309, 0.244 and 0.101 for a five-branch parameterisation using the proposal from Table 3 of Miller and Rice (1983) were adopted. The raw samples are available from the authors if other parameterisations are required by users of this GMM.

The same functional form used for the individual stochastic models was found to fit the samples for the three- and five-branch parameterisations well. Therefore, GMMs were derived using this functional form and nonlinear least-squares regression. The three-branch version is used for the subsequent plots. A comparison between the three- and five-branch versions is shown in the Electronic Supplement. As expected, the central branches are the same in both cases as they both correspond to the median; the outer branches for both versions are very similar as the percentiles targeted are almost identical (5th and 3.5th, and 95th and 96.5th for the three- and five-branch versions, respectively); and the second and fourth branches for the five-branch version are quite close to the central branch.

Figure 9 shows between-event residuals with respect to magnitude from the instrumental data for four spectral periods (0.01, 0.1, 0.5 and 1.0 s) using the weighted mean of the three-branch parameterisation. The weighted mean is used in these plots to test whether the model is well centred, both considering all data and just the UK data (plots for the three separate branches are included in the Electronic Supplement). As expected,

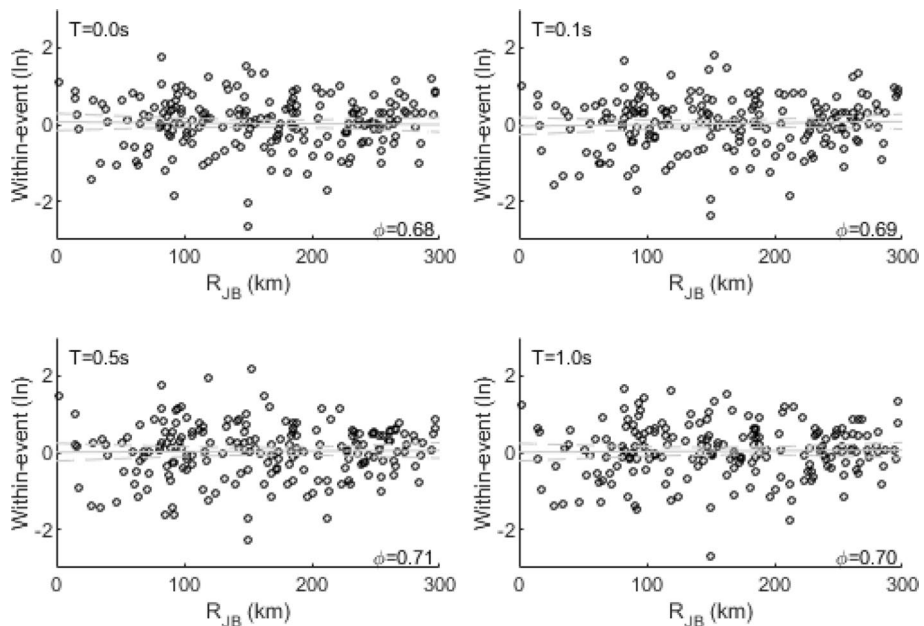


**Fig. 10** Within-event residuals against magnitude for the weighted mean of the three-branch parameterisation of the model. Grey lines are the linear best-fit line and its 95% confidence limits

residuals using the weighted mean show little bias. This is also true for the central (50th percentile) branch. The 5th percentile branch shows positive bias (under-prediction) and the 95th percentile branch shows negative bias (over-prediction). Due to the focus being on larger magnitudes and closer distances than much of the data, we do not consider the minor under-prediction (positive biases between 11 and 30%) for the weighted mean as a significant limitation of the model. Considering only the UK data, the bias is close to zero ( $-2\%$  to  $14\%$ ) for all periods, although this is based on only 11 earthquakes, the largest of which has a magnitude of only  $M$  4.9 (Market Rasen). Similarly to the case for the reweighting, the impact of the site adjustment on the residuals is limited with only a change in bias of a maximum of 3% between adjusting and not adjusting for differences in  $V_{S30}$ .

Figure 10 shows within-event residuals with respect to distance for the weighted mean (graphs for the individual branches are similar, see Electronic Supplement). The weighted mean and none of the branches show clear trends in terms of magnitude or distance, which suggests that the hybrid model correctly captures the magnitude and distance scaling of UK ground motions. Additionally, there are limited trends with respect to focal depth (Fig. 11), although there is some evidence of slight overprediction (negative residuals) of the shallowest events (depth  $< 7$  km).

The use of magnitude-independent stress drops (based on the fit with GMPEs for  $M > 5.5$ , Sect. 3.9) does not introduce trends into the model for  $M < 5.5$ . It should be noted, however, that the instrumental data are limited mainly to  $M < 5$  and  $R > 100$  km and hence these residual plots, although reassuring that the available observations are well predicted, do not mean that ground motions from larger earthquakes and short

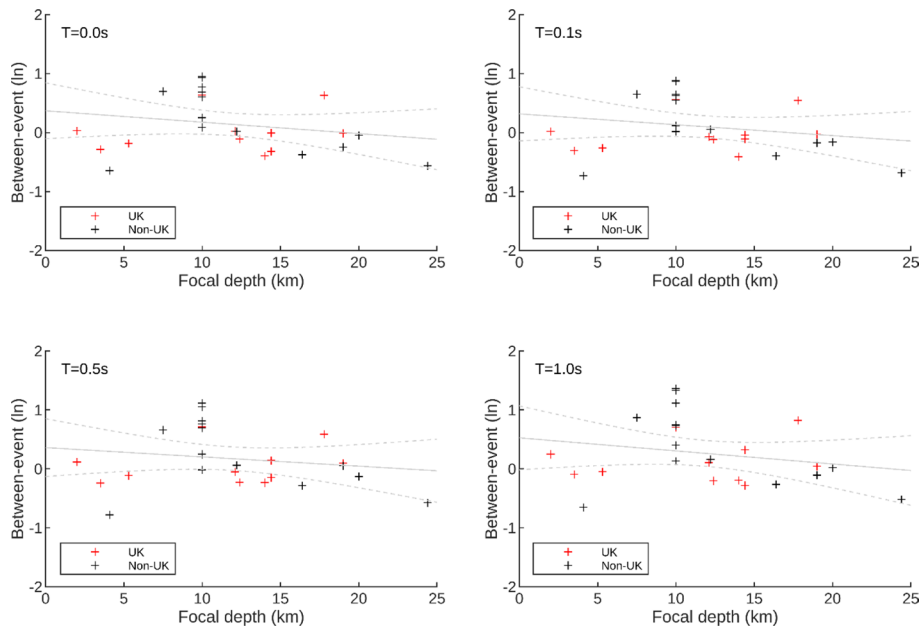


**Fig. 11** Between-event residuals, separated into events located in the UK and those located in the wider region, against focal depth for the central branch of the three-branch parameterisation of the model. Grey lines are the linear best-fit line and its 95% confidence limits

distances are necessarily well predicted. This is the reason why the epistemic uncertainties remain high (see Sect. 5.1).

### 4.3 Comparison with other observations

The high-quality instrumental data collected for this study are limited in terms of magnitude and distance coverage to mainly  $M < 5$  and  $R_{\text{epi}} > 100$  km. Therefore, the magnitude-distance range of main interest for engineering purposes is poorly sampled. Additional instrumental data from the UK and surrounding region, not used to derive the model, were collected from earthquakes  $M > 5$  to check the model for this magnitude range. These data were obtained from: North Sea 1927 ( $M 5.2$ ), Dogger Bank 1931 ( $M 5.9$ , BGS<sup>6</sup>), Norwegian Sea 1988 ( $M 5.6$ ), North Sea 1989 ( $M 5.1$ <sup>7</sup>) and Roermond 1992 ( $M 5.3$ ) earthquakes from Bungum et al. (2003) and the ESM database (Luzi et al. 2020). These data are of lower quality (particularly records from the 1927 and 1931 events) than the data used to reweight the model above and they are all from  $R_{\text{epi}} > 80$  km. In addition, the data from Bungum et al. (2003) were not recorded on strong-motion instruments so only longer period ( $T > 0.5$  s) PSAs can be computed. Nevertheless, as these provide additional checks on the model for the magnitude range of interest to most end users they are considered here. Figure 12 shows that the predictions and the 15 observations match reasonably

<sup>6</sup> Bungum et al. (2003) report  $M 5.3$  for this event but this is inconsistent with the  $M_L 6.1$  reported by BGS.

<sup>7</sup> Converted using Eq. 22 of Scordilis (2006) from  $m_b 4.8$  (ISC).

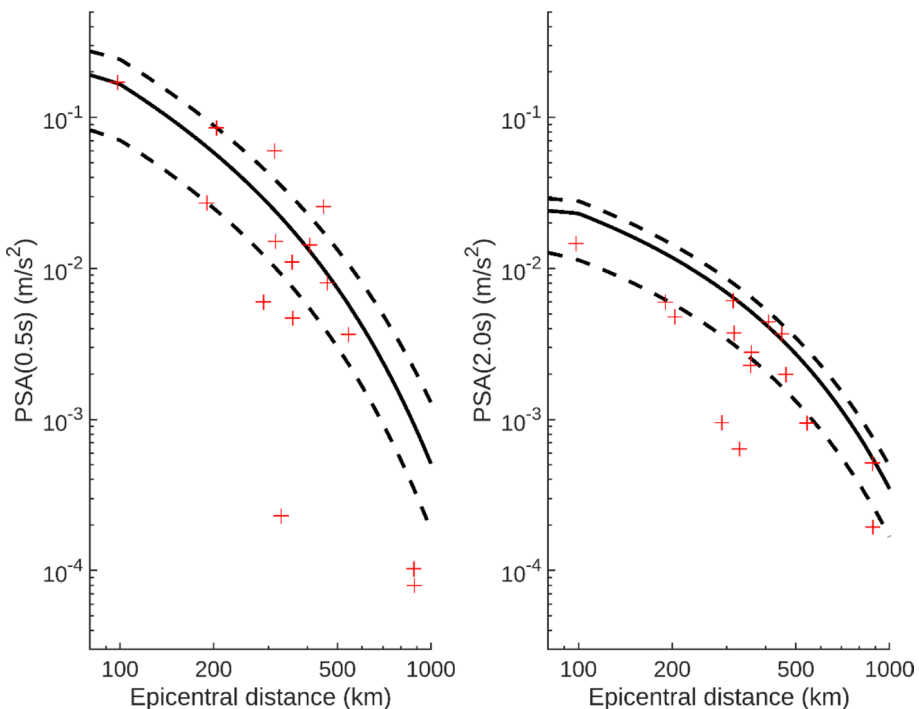


**Fig. 12** Predictions from the backbone-version of the GMM for M5.5 and 15 observed PSAs (adjusted using the GMM's predictions for M 5.5 and each event's magnitude) at 0.5 s (left) and 2.0 s (right) that were not used to derive the model

closely, even at greater distances ( $R_{\text{epi}} > 300$  km) where the model is based only on stochastic estimates. There is evidence that the GMM overpredicts these sparse observations but given the sparse data we propose no adjustment to the GMM to account for this.

Another type of data that can be used as a check on the GMM for the critical larger magnitude range ( $M > 5$ ) are macroseismic intensity observations. As the GMM provides predictions in terms of elastic response spectral accelerations, these accelerations need to be converted to macroseismic intensities for comparisons with this type of observation. We follow Delavaud et al. (2009) and Villani et al. (2019) in converting predictions from the model to corresponding intensities rather than the observed intensities to estimated spectral accelerations. To make this conversion it is necessary to use a ground-motion-to-intensity conversion equation (GMICE), many of which have been published in the past 50 years. For this study, we adopted the GMICE of Dangkua and Cramer (2011), which was developed using data from CENA and California and shows good correlation with UK PGA-intensity pairs.

The focus in this section is on checking the model for ground motions of engineering interest; thus, only earthquakes in the ground-motion database (see Sect. 3.1) with  $M > 4.5$  have been considered here. Dangkua and Cramer (2011) provide GMICEs for PGA, peak ground velocity and pseudo-spectral accelerations at 0.5, 1.0 and 3.3 Hz; however, only the correlation between PGA (assumed equal to PSA at 0.01 s) and intensity is used for this comparison. Figure 13 presents comparisons of the predictions from the lower, middle and

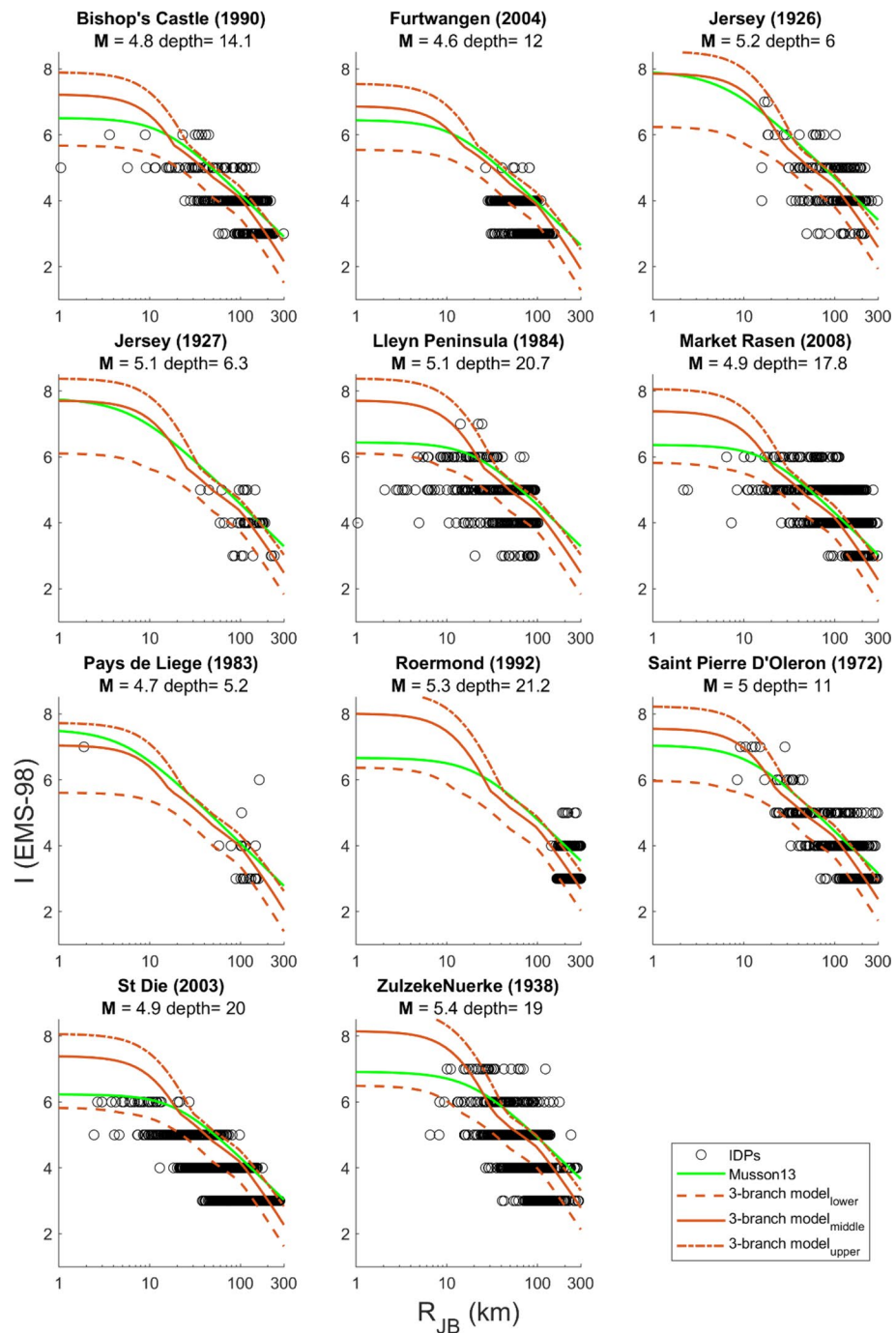


**Fig. 13** Comparison of the predictions from the lower, middle and upper branches of the three-branch parameterisation of the model [converted to intensity using the Dangkua and Cramer (2011) GMICE] with macroseismic data and predictions of the Musson (2013) IPE for earthquakes with  $M > 4.5$

upper branches of the three-branch model, converted to intensities, with intensity data for events from the UK and adjacent regions. These comparisons also include predictions from the intensity prediction equation (IPE) of Musson (2013) which was derived specifically for the UK.

In general, a good correlation of the intensities converted from the middle branch is observed with the data and predictions from the Musson (2013) IPE, particularly for  $R_{JB} > 30$  km. Also, the lower and upper branches of the three-branch model capture the uncertainty reasonably well, noting that the uncertainty increases significantly at  $R_{JB} < 30$  km, where data are scarce.

## 5 Comparison with other models used in UK hazard assessments

In this section various comparisons are shown amongst the three-branch version of the GMM using  $R_{JB}$  and models commonly used for seismic hazard assessments in the UK. The models chosen are: PML (1988) [PML88], because of its historical use within the UK nuclear industry; the Rietbrock and Edwards (2019) model [RE19], as this is the most recent published model for the UK [of the three alternative versions of this model (i.e., 5, 10 and 20 MPa) the 5 MPa version is used here as it was found by Aldama-Bustos et al. (2023) to better agree with UK data]; and the GMM proposed by Aldama-Bustos et al. (2023) for SZC.

Plots showing the distance (Fig. 14) and magnitude (Fig. 15) scaling of the models are drawn as well as predicted response spectra for four earthquake scenarios (Fig. 16). Note that Figs. 14 and 15 show the weighted mean predictions from the three-branch parameterisation of the backbone model, while Fig. 16 shows the three individual branches (lower, middle and upper). Note that all models in these comparisons predict ground motions compatible with the geometric mean of the two horizontal components, except for PML88, which uses the larger of the two horizontal components. To account for this incompatibility, the relationship proposed by Boore and Kishida (2017) was used to convert predictions for the PML88 model from the larger component to the geometric mean.

From the distance and magnitude scaling comparisons (Figs. 14, 15, respectively), generally good agreement is observed between the three-branch backbone model and the SZC GMM and RE19, with the backbone model generally predicting slightly larger ground-motion intensities for most magnitude-distance combinations. The PML88 model predicts consistently larger ground motions at magnitudes  $< M \sim 5.5$  and distances greater than 100 km. The largest differences are observed at around 100 km, where the effects of the Moho "bounce" are strongest. This effect is more evident in the RE19 model (see plateau on the distance scaling, Fig. 14), less so for the SZC and backbone models and absent from PML88.

Similar conclusions are reached from Fig. 16 for the middle branch of the three-branch model. Figure 16 also clearly shows that the epistemic uncertainty captured by the lower and upper branches of the three-branch backbone model comfortably envelopes predictions from all other models. The only exception to this is the PML88 model which predicts higher PSA at  $M 5$  and 100 km. As discussed before, PML88 consistently predicts significantly larger ground-motion intensities for this magnitude-distance scenario. It can be observed that the spectral shape predicted by the upper branch of the model is unusual, with a second peak at around 0.05 s in addition to the usual spectral peak at around 0.2 s. This shape is due to low high-frequency attenuation predicted by the lowest kappa value

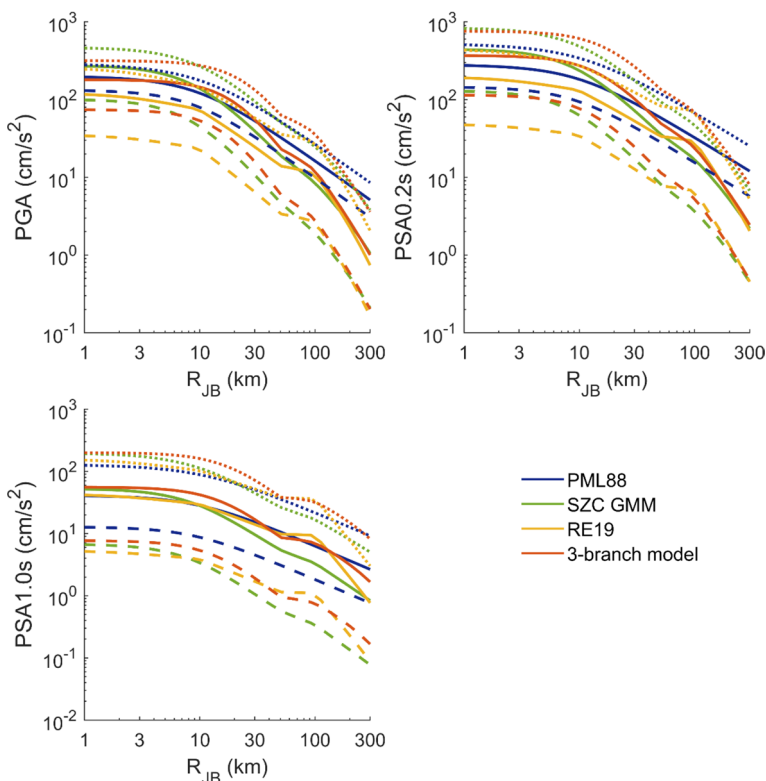


**Fig. 14** Distance scaling for PGA and PSA at 0.2 s and 1.0 s, and magnitudes  $M$  4.5 (dashed lines), 5.5 (solid lines) and 6.5 (dotted lines), for selected GMMs, previously used in seismic hazard assessments for nuclear facilities in the UK, and the three-branch parameterisation of the model (weighted mean from all three branches) in this study

interacting with the site amplification due to the chosen  $V_S$  profile, which has a relatively high amplification at short periods. As this shape has a physical basis, we decided not to apply any period-dependent smoothing to the coefficients.

A final comparison made here is to compare the predicted peak displacements from the stochastic model with those associated with the local magnitude calibration functions used by the BGS for UK earthquakes. To do this, SMSIM was used to evaluate the spectral displacement of a single-degree-of-freedom oscillator with a period of 0.8 s and a critical damping ratio of 0.69, which is stated by Boore (2005) to be equivalent to the Wood-Anderson instrument that is the basis of the local magnitude scale. This was done for the branch of the stochastic model that had the highest weight in the reweighted version (i.e. branch 1 of the  $Z_{TOR}$  model, 80 bars, central geometric spreading, central Q model and  $\kappa=0.023$  s). The local magnitude calibration functions of Hutton and Boore (1987) and Ottemöller and Sargeant (2013), which are used by the BGS, are rearranged to express the spectral displacements as a function of magnitude and distance. The local to moment magnitude conversion equation (their Eq. 9) derived by Ottemöller and Sargeant (2013) is used to convert between moment and local magnitudes for  $M < 5$  (the magnitude range for which it is calibrated). The resulting spectral displacements from the stochastic model and

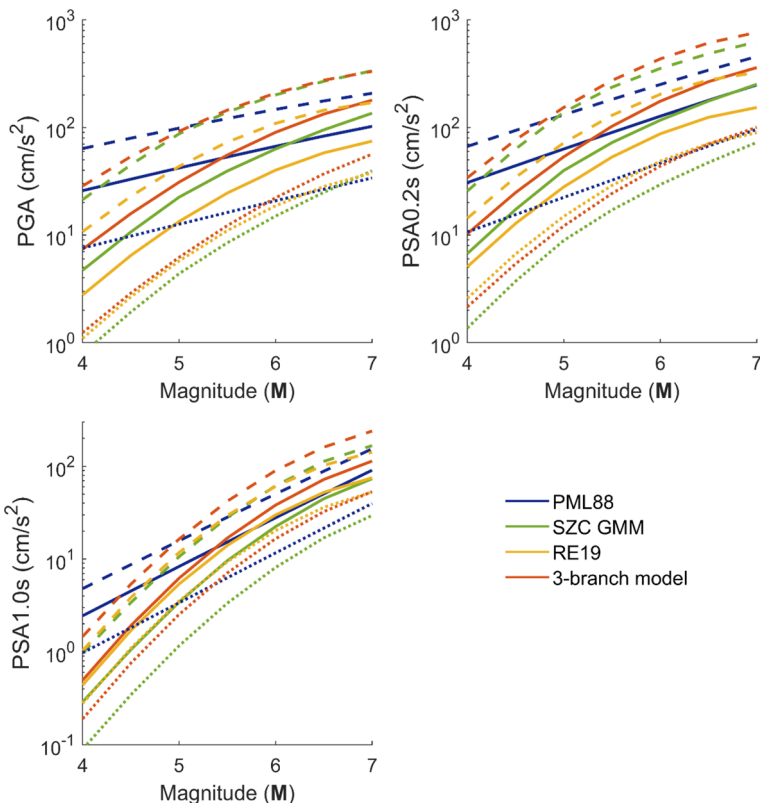


**Fig. 15** Magnitude scaling for PGA and PSA at 0.2 s and 1.0 s, and distances of 10 km (dashed lines), 30 km (solid lines) and 100 km (dotted lines), for selected GMMs, previously used in seismic hazard assessments for nuclear facilities in the UK, and the three-branch parameterisation of the model (weighted mean from all three branches) in this study

local magnitude calibration functions are shown in Fig. 17. The close match between the curves for all magnitudes demonstrates that the highest weighted branch of the stochastic model is broadly consistent with the model used for magnitude calibration for the UK.

## 5.1 Epistemic uncertainty

One of main drivers for the development of the models presented here was the requirement to capture epistemic uncertainty within the prediction of UK ground motions. Therefore, in this section the epistemic uncertainty captured by the GMMs is analysed and compared with that captured by other relevant models. The approach that is used here is to compare contour plots of  $\sigma_{\ln \mu}$  (i.e. the standard deviation of the logarithm of the median predicted spectral accelerations) over magnitude and distance ranges. This approach is one of those discussed by Aldama-Bustos et al. (2023) and is the simplest to visualise given the large number of GMMs and branches considered here.

The impact of the reweighting on  $\sigma_{\ln \mu}$  is shown in Fig. 18 for periods 0.01 s, 0.2 s, 0.5 s and 1 s. The reweighting reduces the values slightly, particularly at greater distances ( $R > 70$  km), which corresponds to where the UK data are concentrated. The

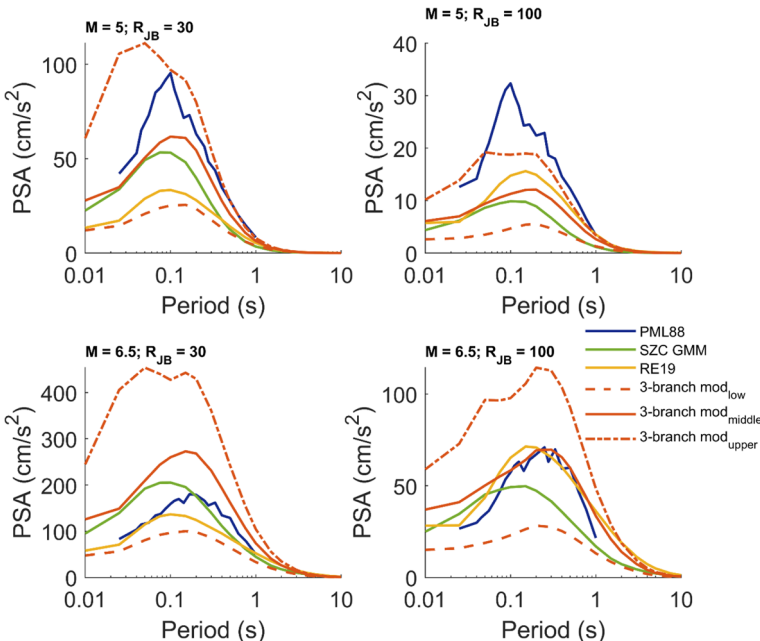


**Fig. 16** Response spectra for  $M$  5.0 and 6.0 at 30 and 100 km for selected GMMs, previously used in seismic hazard assessments for nuclear facilities in the UK, and the backbone model in this study

magnitude-distance dependence of  $\sigma_{\ln \mu}$  is also related to basic seismological theory because the HEM allows information on expected ground motion scaling to be brought in from the empirical model of Chiou and Youngs (2014) and via the stochastic method. For example, the UK data provides some information on average kappa, which reduces uncertainties for all magnitudes and distances and not just where the data are concentrated. Therefore, the epistemic uncertainty is not simply related to the UK data distribution. This explains the strong magnitude dependency of  $\sigma_{\ln \mu}$  at periods of 0.2 s and above, and  $R_{JB} < 70$  km. This is because the single-corner stochastic model adopted means that the influence of uncertainties in stress-drop and path and site attenuation is minimal at small magnitudes and increases with magnitude (there is no uncertainty coming from geometric spreading as all three models assume 1/R decay for near-source distances).

As expected, using the five-branch backbone model leads to similar estimates of  $\sigma_{\ln \mu}$  for all magnitudes and distances (see Electronic Supplement), although there are slight differences because the five-branch model is able to capture more details of the uncertainty distributions. The complete parameterisation (using all 162 branches and associated weights) also leads to similar values of  $\sigma_{\ln \mu}$  for all magnitudes and distances, which shows that the backbone parameterisation does not lead to a significant loss of accuracy despite using far fewer branches.

Using contour plots of  $\sigma_{\ln \mu}$ , the epistemic uncertainties captured in the new model can be compared with those from recent GMMs for the UK. Figure 19 shows  $\sigma_{\ln \mu}$  contours

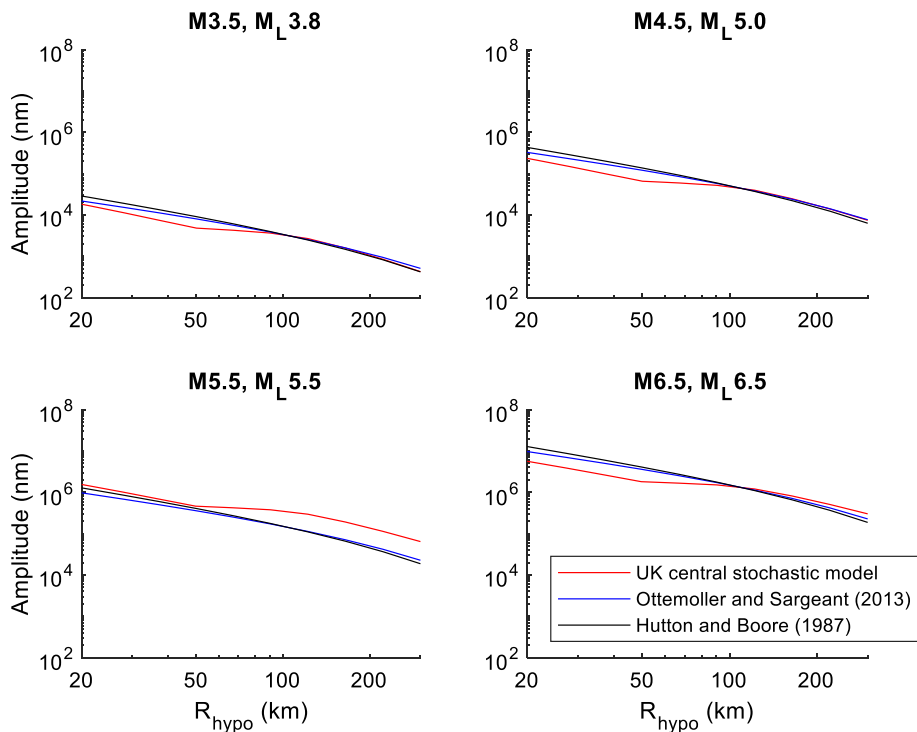


**Fig. 17** Comparison of the spectral displacements estimated from the highest weighted branch of the stochastic model and those estimated from the Hutton and Boore (1987) and Ottemöller and Sargeant (2013) local magnitude calibration functions for  $M = 3.5, 4.5, 5.5$  and  $6.5$

obtained for the SZC GMM (Aldama-Bustos et al. 2023) for periods 0.01 s, 0.2 s, 0.5 s and 1 s, covering the same magnitude and distance ranges as in Fig. 18, for the three-branch backbone model. By comparing Figs. 18 and 19, it can be seen that the epistemic uncertainty captured by the new model is comparable to that in other recent models but that because of the use of the HEM, the uncertainties vary smoothly with magnitude and distance, and they are explainable in terms of seismological theory and available data. The reweighting approach used here would allow the uncertainties of the model to be reduced as more UK ground-motion data are recorded. This provides a rigorous framework for making use of new data.

## 6 Conclusions

In this article the development of a ground-motion model for the prediction of median elastic response spectral accelerations from earthquakes occurring in the UK and surrounding region was presented. For probabilistic seismic hazard assessments, a median ground-motion model needs to be coupled with a model of the aleatory variability (i.e., sigma) of the ground motions. Given that the limited data available for the UK and surrounding regions do not allow the derivation of a reliable sigma model, we suggest considering previously published models (e.g., Al Atik 2015) for this component. The

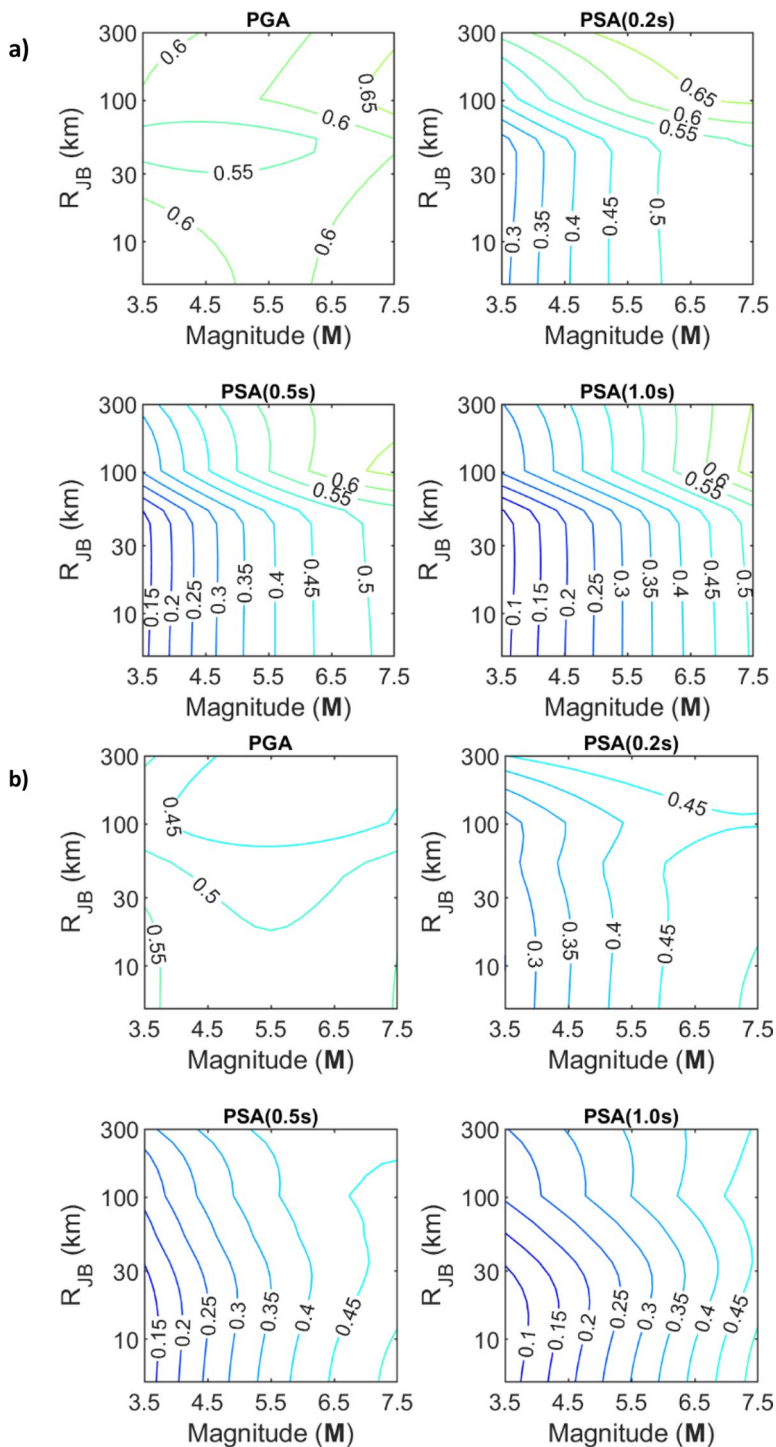


**Fig. 18** Contour plots of  $\sigma_{\ln \mu}$  for the three-branch backbone: a) using the *a priori* weights and b) using the adjusted weights, for 0.01 s (PGA), 0.2 s, 0.5 s and 1.0 s

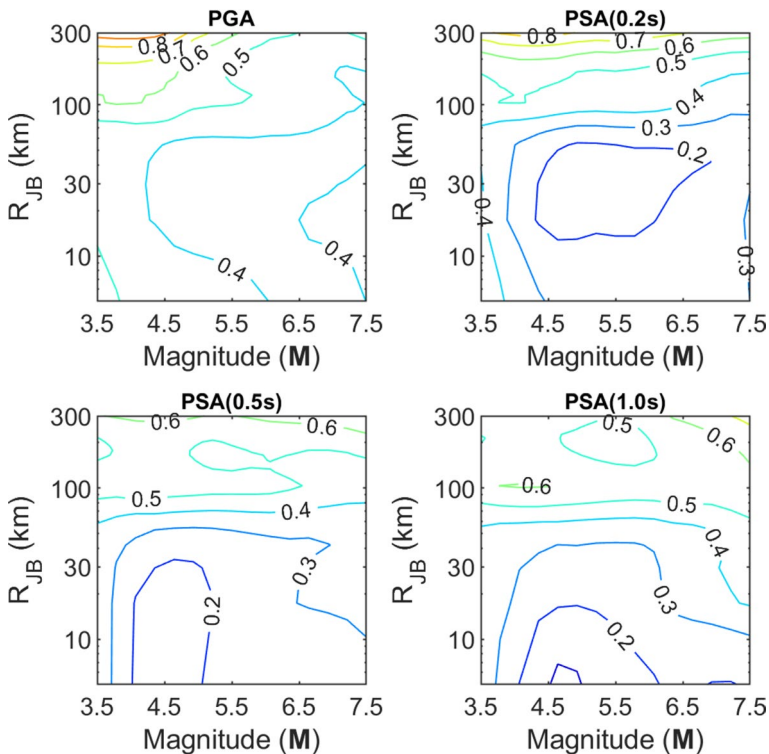


**Fig. 19** Contours of  $\sigma_{\ln \mu}$  for the SZC GMM, for 0.01 s, 0.2 s, 0.5 s and 1.0 s

main advantage of the Al Atik's (2015) models over other recent models is that they explicitly account for the epistemic uncertainty and are informed by the predictions from four of the NGA-West2 models, including Chiou and Youngs (2014) [i.e., Abrahamson et al. (2014), Boore et al. (2014), Campbell and Bozorgnia (2014) and Chiou and Youngs (2014)]. Additionally, Al Atik (2015) provides ergodic and single-station sigma models for "central and eastern North America" and "Global" regions. We recommend that the hazard analyst carefully considers the most appropriate sigma model for their application.

The backbone model presented in this article accounts for epistemic uncertainties due to the depth distribution of UK earthquakes, geometric spreading, path attenuation, site attenuation and stress drop, which are the most important sources of uncertainty within the hybrid empirical-stochastic method that has been adopted. All inputs to the model development were chosen/estimated based on previous publications and analysis of data from the UK and surrounding region. The model was justified through comparisons with available instrumental and macroseismic data, as well as comparisons with models previously proposed for use in the UK.

The epistemic uncertainties captured by the model were further illustrated and discussed. It was shown that these epistemic uncertainties are similar to those in recent high-level seismic hazard assessments for nuclear facilities and that they follow what would be expected: lower uncertainties where there are data and higher uncertainties

where data are lacking. Therefore, we argue that the model captures the centre, body and range of the technically defensible interpretations.

A comparison of the predictions from this model with those from other models used in seismic hazard assessments for the UK shows generally good agreement, apart from with the model of PML (1988), which behaves in a different manner from all other models used in the comparisons for magnitudes  $M < 5.5$  and distances greater than 100 km.

We recommend that the reweighted three-branch backbone version of the model (either using  $R_{JB}$  or  $R_{RUP}$ ) be used for seismic hazard assessments in the UK and surrounding offshore region for  $M$  3.5 to 7.25, for source-to-site distances up to 1000 km and for rock sites with  $V_{S30}$  around 900 m/s. For some applications (e.g. site-specific or research studies), other parameterisations (five-branch and 162-branch versions) and weightings (*a priori* and reweighted), which have the same ranges of applicability, are provided for completeness.

The strengths of the developed ground-motion models include: the explicit capturing of uncertainties in key input parameters, predictions that are constrained by both seismological theory and empirical data and hence are realistic over a wide magnitude-distance space, and parameterisation of model predictions in an easy-to-use form that capture epistemic uncertainties. The models do have the following limitations: key inputs (particularly, kappa and stress drop) remain poorly constrained due to limited data from earthquakes with  $M > 5$  and uncertain corrections for local site effects, long-period ( $T > 2$  s) predictions may require adjustments because of limitations with the empirical model, and the functional form employed may not capture all details of the ground-motion predictions.

**Supplementary Information** The online version contains supplementary material available at <https://doi.org/10.1007/s10518-024-01943-8>.

**Acknowledgements** We thank all those who provided comments following: the SECED Evening Meeting on 25th January 2023 (<https://youtu.be/lKHy3oupIcA?si=nhcggw9bVVmTf5B8>), the SECED Conference presentation on 14th September 2023, an internal seminar on 15th November 2023 and the SECED Evening Meeting on 28th February 2024 (<https://youtu.be/nhTCD7Bgzxo?si=EB46iy4lsMgOfm3w>) on this project. We also thank the seismic networks, especially the British Geological Survey, Hilmar Bungum and Conrad Lindholm for providing the ground-motion records used here. We thank David M. Boore for his valuable help in using SMSIM. We are grateful to Fleur O. Strasser for her valuable input early in the model development. Finally, we thank Gabriele Ameri, Julian Bommer and an anonymous reviewer for their detailed and constructive comments on a previous version of this manuscript.

**Author contributions** All authors contributed to the study conception and design. Data collection and analysis were performed by John Douglas, Guillermo Aldama-Bustos, Sarah Tallett-Williams and Manuela Daví. Original simulations were performed by John Douglas. Results were discussed by all authors. Final simulations were performed by John Douglas. Analysis of the results was performed by John Douglas and Guillermo Aldama-Bustos. The first draft of the manuscript was written by John Douglas. All authors commented on this draft and contributed to writing the final manuscript. All authors read and approved the final manuscript. All authors contributed to revisions of the manuscript.

**Funding** The work presented here was supported by a Fellowship held by the lead author and funding from Jacobs. This Fellowship was supported by the Royal Academy of Engineering (Grant No. IF2223-160) under their Industrial Fellowships programme.

**Data availability** Outputs from CHEEP used in this research and software codes to evaluate the ground-motion models are accessible. GitHub ([https://github.com/aldabus/DouglasEtAl\\_UK\\_HEM\\_GMM](https://github.com/aldabus/DouglasEtAl_UK_HEM_GMM)).

## Declarations

**Conflict of interest** The authors declare that they have no conflict of interest.

**Open Access** This article is licensed under a Creative Commons Attribution 4.0 International License, which permits use, sharing, adaptation, distribution and reproduction in any medium or format, as long as you give appropriate credit to the original author(s) and the source, provide a link to the Creative Commons licence, and indicate if changes were made. The images or other third party material in this article are included in the article's Creative Commons licence, unless indicated otherwise in a credit line to the material. If material is not included in the article's Creative Commons licence and your intended use is not permitted by statutory regulation or exceeds the permitted use, you will need to obtain permission directly from the copyright holder. To view a copy of this licence, visit <http://creativecommons.org/licenses/by/4.0/>.

## References

- Abrahamson NA, Silva WJ, Kamai R (2014) Summary of the ASK14 ground motion relation for active crustal regions. *Earthquake Spectra* 30(3):1025–1055
- Akkar S, Sandikkaya MA, Ay BÖ (2014) Compatible ground-motion prediction equations for damping scaling factors and vertical-to-horizontal spectral amplitude ratios for the broader Europe region. *Bull Earthq Eng* 12:517–547
- Al Atik L (2015) NGA-East: ground-motion standard deviation models for central and eastern North America. *Pac Earthq Eng Res Center PEER Rep* 2015(07):217
- Al Atik L, Abrahamson N (2021) A methodology for the development of 1D reference  $V_S$  profiles compatible with ground-motion prediction equations: application to NGA-West2 GMPEs. *Bull Seismol Soc Am* 111(4):1765–1783
- Al Atik L, Kottke A, Abrahamson N, Hollenback J (2014) Kappa ( $\kappa$ ) scaling of ground-motion prediction equations using an inverse random vibration theory approach. *Bull Seismol Soc Am* 104(1):336–346
- Aldama-Bustos G and Strasser F (2019) On the strong-motion duration of UK earthquakes. In: SECED 2019 conference—earthquake risk and engineering towards a resilient world. Society for Earthquake and Civil Engineering Dynamics, Greenwich
- Aldama-Bustos G, Douglas J, Strasser FO, Daví M, MacGregor A (2023) Methods for assessing the epistemic uncertainty captured in ground-motion models. *Bull Earthq Eng* 21(1):1–26
- Ambraseys NN, Jackson JA (1985) Long-term seismicity in Britain. In: *Earthquake engineering in Britain*, pp 49–66. Thomas Telford, London
- Anderson JG, Hough SE (1984) A model for the shape of the Fourier amplitude spectrum of acceleration at high frequencies. *Bull Seismol Soc Am* 74:1969–1993
- Atkinson GM, Silva W (2000) Stochastic modeling of California ground motions. *Bull Seismol Soc Am* 90(2):255–274
- Atkinson GM, Bommer JJ, Abrahamson NA (2014) Alternative approaches to modeling epistemic uncertainty in ground motions in probabilistic seismic-hazard analysis. *Seismol Res Lett* 85:1141–1144
- Baptie B (2010) Seismogenesis and state of stress in the UK. *Tectonophysics* 482(1–4):150–159
- Baptie B (2021) Earthquake seismology 2020/2021. British Geological Survey Open Report, OR/21/033
- Bayless J, Abrahamson NA (2019) Summary of the BA18 ground-motion model for Fourier amplitude spectra for crustal earthquakes in California. *Bull Seismol Soc Am* 109:2088–2105
- BCSF (2022) Le Bureau Central Sismologique Français—BCSF. <http://www.franceseisme.fr/english.php>
- BGS (2022a) BGS earthquake database search. <http://quakes.bgs.ac.uk/earthquakes/dataSearch.html>
- BGS (2022b) UK historical earthquake database. [https://earthquakes.bgs.ac.uk/historical/query\\_eq/](https://earthquakes.bgs.ac.uk/historical/query_eq/) (2022/01/27)
- Bindi D, Massa M, Luzzi L, Ameri G, Pacor F, Puglia R, Augliera P (2014) Pan-European ground motion prediction equations for the average horizontal component of PGA, PGV, and 5%-damped PSA at spectral periods up to 3.0 s using the RESORCE dataset. *Bull Earthq Eng* 12:391–430
- Boatwright J (1978) Detailed spectral analysis of two small New York State earthquakes. *Bull Seismol Soc Am* 68:1117–1131
- Bommer JJ (2024) Evolution of the backbone approach to building ground-motion logic trees for site-specific PSHA. In: Proceedings of the 18th world conference on earthquake engineering, Milan, Italy
- Bommer JJ, Stafford PJ (2020) Selecting ground-motion models for site-specific PSHA: adaptability versus applicability. *Bull Seismol Soc Am* 110(6):2801–2815
- Bommer JJ, Stafford PJ, Alarcon JE, Akkar S (2007) The influence of magnitude range on empirical ground-motion prediction. *Bull Seismol Soc Am* 97(6):2152–2170
- Bommer JJ, Stafford PJ, Alarcon JE (2009) Empirical equations for the prediction of the significant, bracketed, and uniform duration of earthquake ground motion. *Bull Seismol Soc Am* 99(6):3217–3233

- Bommer JJ, Stafford PJ, Ruigrok E, Rodriguez-Marek A, Ntinalexis M, Kruiver PP, Edwards B, Dost B, van Elk J (2022) Ground-motion prediction models for induced earthquakes in the Groningen gas field, The Netherlands. *J Seismol* 26:1157–1184
- Boore DM (2003) Simulation of ground motion using the stochastic method. *Pure Appl Geophys* 160:635–676
- Boore DM (2005) SMSIM—Fortran programs for simulating ground motions from earthquakes: version 2.3—a revision of OFR 96-80-A. A modified version of OFR 00—509, describing the program as of 15 August, 2005 (version 2.30). US Geological Survey
- Boore DM (2016) Determining generic velocity and density models for crustal amplification calculations, with an update of the Boore and Joyner (1997) generic site amplification for m/s. *Bull Seismol Soc Am* 106(1):313–317
- Boore DM, Kishida T (2017) Relations between some horizontal-component ground-motion intensity measures used in practice. *Bull Seismol Soc Am* 107(1):334–343
- Boore DM, Thompson EM (2014) Path durations for use in the stochastic-method simulation of ground motions. *Bull Seismol Soc Am* 104(5):2541–2552
- Boore DM, Thompson EM (2015) Revisions to some parameters used in stochastic-method simulations of ground motion. *Bull Seismol Soc Am* 105(2A):1029–1041
- Boore DM, Stewart JP, Seyhan E, Atkinson GM (2014) NGA-West2 equations for predicting PGA, PGV, and 5% damped PSA for shallow crustal earthquakes. *Earthquake Spectra* 30(3):1057–1085
- Boore DM, Youngs RR, Kottke AR, Bommer JJ, Darragh R, Silva WJ, Stafford PJ, Al Atik L, Rodriguez-Marek A, Kaklamanos J (2022) Construction of a ground-motion logic tree through host-to-target region adjustments applied to an adaptable ground-motion prediction model. *Bull Seismol Soc Am* 112(6):3063–3080
- BRGM, EDF and IRSN (2022) SisFrance Sismicité historique de la France. <https://www.sisfrance.net/seismes>
- Brune JN (1970) Tectonic stress and the spectra of seismic shear waves from earthquakes. *J Geophys Res* 75:4997–5009
- Brune JN (1971) Correction. *J Geophys Res* 76:5002–5002
- Bungum H, Dahle A, Toro G, McGuire R, Gudmestad OT (1992) Ground motions from intraplate earthquakes. *Proc Tenth World Conf Earthq Eng* 2:611–616
- Bungum H, Lindholm CD, Dahle A (2003) Long-period ground-motions for large European earthquakes, 1905–1992, and comparisons with stochastic predictions. *J Seismolog* 7:377–396
- Campbell KW (2003) Prediction of strong ground motion using the hybrid empirical method and its use in the development of ground-motion (attenuation) relations in eastern North America. *Bull Seismol Soc Am* 93:1012–1033
- Campbell KW, Bozorgnia Y (2014) NGA-West2 ground motion model for the average horizontal components of PGA, PGV, and 5% damped linear acceleration response spectra. *Earthq Spectra* 30(3):1087–1115
- Campillo M, Plantier JL (1991) Frequency dependence and spatial distribution of seismic attenuation in France: experimental results and possible interpretations. *Phys Earth Planet Inter* 67:48–64
- Cauzzi C, Faccioli E, Vanini M, Bianchini A (2015) Updated predictive equations for broadband (0.01–10 s) horizontal response spectra and peak ground motions, based on a global dataset of digital acceleration records. *Bull Earthq Eng* 13:1587–1612
- Chiou BS-J, Youngs RR (2014) Update of the Chiou and Youngs NGA model for the average horizontal component of peak ground motion and response spectra. *Earthq Spectra* 30:1117–1153
- Cotton F, Scherbaum F, Bommer JJ, Bungum H (2006) Criteria for selecting and adjusting ground-motion models for specific target regions: application to central Europe and rock sites. *J Seismol* 10(2):137–156
- Dangkua DT, Cramer CH (2011) Felt intensity versus instrumental ground motion: A difference between California and eastern North America? *Bull Seismol Soc Am* 101(4):1847–1858
- Delavaud E, Scherbaum F, Kuehn N, Riggelsen C (2009) Information-theoretic selection of ground-motion prediction equations for seismic hazard analysis: an applicability study using Californian data. *Bull Seismol Soc Am* 99(6):3248–3263
- Delavaud E, Cotton F, Akkar S et al (2012) Toward a ground-motion logic tree for probabilistic seismic hazard assessment in Europe. *J Seismolog* 16:451–473
- Douglas J (2018) Capturing geographically-varying uncertainty in earthquake ground motion models or what we think we know may change. *Recent Adv Earthq Eng Europe Geotech Geol Earthq Eng* 46:153–181
- Douglas J, Bungum H, Scherbaum F (2006) Ground-motion prediction equations for southern Spain and southern Norway obtained using the composite model perspective. *J Earthq Eng* 10(1):33–72

- Douglas J, Strasser FO, Aldama-Bustos G, Tallett-Williams S, Daví M and Tromans IJ (2023) Development of a suite of stochastic ground-motion models for the United Kingdom. In: SECED 2023 conference—earthquake engineering and dynamics for a sustainable future. Society for Earthquake and Civil Engineering Dynamics, Cambridge. <https://www.seced.org.uk/index.php/seced-2023-proceedings>
- Drouet S, Cotton F (2015) Regional stochastic GMPEs in low-seismicity areas: scaling and aleatory variability analysis—application to the French Alps. *Bull Seismol Soc Am* 105(4):1883–1902
- Drouet S, Ameri G, Le Dortz K, Secanell R, Senfaute G (2020) A probabilistic seismic hazard map for the metropolitan France. *Bull Earthq Eng* 18:1865–1898
- Edwards B, Fäh D (2013) A stochastic ground-motion model for Switzerland. *Bull Seismol Soc Am* 103(1):78–98
- Edwards B, Rietbrock A, Bommer JJ, Baptie B (2008) The acquisition of source, path, and site effects from microearthquake recordings using Q tomography: application to the United Kingdom. *Bull Seismol Soc Am* 98:1915–1935
- EPRI (2004), CEUS Ground Motion Project Final Report, EPRI, Palo Alto, CA, Dominion Energy, Glen Allen, VA, Entergy Nuclear, Jackson, MS, and Exelon Generation Company, Kennett Square, PA: 2004, p 1009684
- Galloway DD (2021) The British Geological Survey Earthquake Bulletin for 2020. BGS Internal Report, OR/21/005, British Geological Survey.
- Goda K, Aspinall W, Taylor CA (2013) Seismic hazard analysis for the U.K.: sensitivity to spatial seismicity modelling and ground motion prediction equations. *Seismol Res Lett* 84(1):112–129
- Goutbeek FH, Dost B, van Eck T (2004) Intrinsic absorption and scattering attenuation in the southern part of The Netherlands. *J Seismolog* 8:11–23
- Grünthal G, Stromeyer D, Bosse C, Cotton F, Bindi D (2018) The probabilistic seismic hazard assessment of Germany—version 2016, considering the range of epistemic uncertainties and aleatory variability. *Bull Earthq Eng* 16:4339–4395
- Hutton LK, Boore DM (1987) The  $M_L$  in southern California. *Bull Seismol Soc Am* 77(6):2074–2094
- Joyner WB (1984) A scaling law for the spectra of large earthquakes. *Bull Seismol Soc Am* 74:1167–1188
- Kaklamanos J, Baise LG, Boore DM (2011) Estimating unknown input parameters when implementing the NGA ground-motion prediction equations in engineering practice. *Earthq Spectra* 27(4):1219–1235
- Keefer DL, Bodily SE (1983) Three-point approximations for continuous random variable. *Manag Sci* 29(5):595–609
- Kvamme LB, Hansen RA, Bungum H (1995) Seismic-source and wave-propagation effects of Lg waves in Scandinavia. *Geophys J Int* 120:525–536
- Laske G, Masters G, Ma Z, Pasyanos M (2013) Update on CRUST1.0—a 1-degree global model of Earth's crust. *Geophys Res Abstr* 15:Abstract EGU2013-2658
- Leonard M (2014) Self-consistent earthquake fault-scaling relations: update and extension to stable continental strike-slip faults. *Bull Seismol Soc Am* 104(6):2953–2965
- Lubkowski Z, Bommer J, Baptie B, Bird J, Douglas J, Free M, Hancock J, Sargeant S, Sartain N and Strasser F (2004) An evaluation of attenuation relationships for seismic hazard assessment in the UK. In: Proceedings of thirteenth world conference on earthquake engineering. Paper no. 1422
- Luzi L, Lanzano G, Felicetta C, D'Amico MC, Russo E, Sgobba S, Pacor F, ORFEUS Working Group 5 (2020) Engineering strong motion database (ESM) (Version 2.0). Istituto Nazionale di Geofisica e Vulcanologia (INGV). <https://doi.org/10.13127/ESM.2>
- Mai PM, Spudich P, Boatwright J (2005) Hypocenter locations in finite-source rupture models. *Bull Seismol Soc Am* 95(3):965–980
- Main IG, Irving D, Musson R, Reading A (1999) Constraints on the frequency-magnitude relation and maximum magnitudes in the UK from observed seismicity and glacio-isostatic recovery rates. *Geophys J Int* 137:535–550
- Manchuel K, Traversa P, Baumont D, Cara M, Nayman E, Durouchoux C (2018) The French seismic CATalogue (FCAT-17). *Bull Earthq Eng* 16:2227–2251
- Martin C, Ameri G, Baumont D, Carbon D, Senfaute G, Thiry J-M, Faccioli E, Savy J (2018) Probabilistic seismic hazard assessment for south-eastern France. *Bull Earthq Eng* 16:2477–2511
- Miller AC, Rice TR (1983) Discrete approximations of probability distributions. *Manag Sci* 29(3):352–362
- Mosca I, Sargeant S, Baptie B, Musson RMW, Pharaoh TC (2022) The 2020 national seismic hazard model for the United Kingdom. *Bull Earthq Eng* 20:633–675

- Musson RMW (2013) Updated intensity attenuation for the UK, Open Report, OR/13/029, Earth Hazards and Systems Programme
- Ottemöller L, Sargeant S (2010) Ground-motion difference between two moderate-size earthquakes in the UK. *Bull Seismol Soc Am* 100:1823–1829
- Ottemöller L, Sargeant S (2013) A local magnitude scale  $M_L$  for the United Kingdom. *Bull Seismol Soc Am* 103(5):2884–2893
- Ottemöller L, Baptie B, Smith NJP (2009) Source parameters for the 28 April 2007 Mw 4.0 earthquake in Folkestone, United Kingdom. *Bull Seismol Soc Am* 99(3):1853–1867
- PEER (2015) NGA-East: adjustments to median ground-motion models for central and eastern North America. Pacific Earthquake Engineering Research Center, PEER Report No. 2015/08
- PML (1988) UK uniform risk spectra. Technical Report HPC-IP-096013, Principia Mechanica Ltd., London. Report for National Nuclear Corporation
- Poggi V, Edwards B, Fäh D (2011) Derivation of a reference shear-wave velocity model from empirical site amplification. *Bull Seismol Soc Am* 101:258–274
- RESIF (1995a) RESIF-RAP French Accelerometric Network. RESIF—Réseau Sismologique et géodésique Français, <https://doi.org/10.15778/RESIF.RA>
- RESIF (1995b) RESIF-RLBP French Broad-band network. RESIF-RAP strong motion network and other seismic stations in metropolitan France. <https://rlbp.resif.fr/>
- RESIF (2022) RESIF seismic data portal. <http://ws.resif.fr/resifws/timeseries/>
- Rezaeian S, Bozorgnia Y, Idriss IM, Abrahamson N, Campbell K, Silva W (2014) Damping scaling factors for elastic response spectra for shallow crustal earthquakes in active tectonic regions: “average” horizontal component. *Earthq Spectra* 30(2):939–963
- Rietbrock A, Edwards B (2017) Wylya seismic hazard consultancy project. Report Number 1619&2082, Version 2.3, University of Liverpool, June 2017
- Rietbrock A, Edwards B (2019) Update of the UK stochastic ground motion model using a decade of broad-band data. In: 2019 SECED conference
- Rietbrock A, Strasser F, Edwards B (2013) A stochastic earthquake ground-motion prediction model for the United Kingdom. *Bull Seismol Soc Am* 103:57–77
- ROB (2022) Royal observatory of Belgium—seismology-gravimetry. <http://seismologie.oma.be/en>
- Sargeant SL, Ottemöller L (2009) Lg wave attenuation in Britain. *Geophys J Int* 179:1593–1606
- Scherbaum F, Bommer JJ, Bungum H, Cotton F, Abrahamson NA (2005) Composite ground-motion models and logic trees: methodology, sensitivities, and uncertainties. *Bull Seismol Soc Am* 95(5):1575–1593
- Scherbaum F, Delavaud E, Riggelsen C (2009) Model selection in seismic hazard analysis: an information-theoretic perspective. *Bull Seismol Soc Am* 99(6):3234–3247
- Schulte SM, Mooney WD (2005) An updated global earthquake catalogue for stable continental regions: reassessing the correlation with ancient rifts. *Geophys J Int* 161(3):707–721
- Scordilis EM (2006) Empirical global relations converting  $M_S$  and  $m_b$  to moment magnitude. *J Seismol* 10:225–236
- Stafford PJ, Boore DM, Youngs RR, Bommer JJ (2022) Host-region parameters for an adjustable model for crustal earthquakes to facilitate the implementation of the backbone approach to building ground-motion logic trees in probabilistic seismic hazard analysis. *Earthq Spectra* 38(2):917–949
- Tallett-Williams S (2017) Site classification for seismic hazard assessment in low seismicity regions, Ph.D. Thesis, Imperial College London, United Kingdom
- Tromans JJ, Aldama-Bustos G, Douglas J, Lessi-Cheimariou A, Hunt S, Daví M, Musson RMW, Garrard G, Strasser FO, Robertson C (2019) Probabilistic seismic hazard assessment for a new-built nuclear power plant in the UK. *Bull Earthq Eng* 17(1):1–36
- Turbitt T (1984) Catalogue of British Earthquakes recorded by the BGS seismograph network 1979, 1980, 1981. British Geological Survey, Global Seismology Unit, Report number 58
- Van Houtte C, Drouet S, Cotton F (2011) Analysis of the origins of  $\kappa$  (kappa) to compute hard rock to rock adjustment factors for GMPEs. *Bull Seismol Soc Am* 101(6):2926–2941
- Villani M, Polidoro B, McCully R, Ader T, Edwards B, Rietbrock A, Lubkowski Z, Courtney TJ, Walsh M (2019) A selection of GMPEs for the United Kingdom based on instrumental and macroseismic data sets. *Bull Seismol Soc Am* 109:1378–1400
- Villani M, Lubkowski Z, Free M, Musson RMW, Polidoro B, McCully R, Koskosidi A, Oakman C, Courtney T, Walsh M (2020) A probabilistic seismic hazard assessment for Wylya Newydd, a new nuclear site in the United Kingdom. *Bull Earthq Eng* 18(9):4061–4089
- Winter PW (1995) A stochastic ground motion model for UK earthquakes. Technical Report GNSR(DT)/P(96)275 Milestone ECS 0263, AEA/16423530/R003, AEA Technology

- Yenier E, Atkinson GM (2015) Regionally adjustable generic ground-motion prediction equation based on equivalent point-source simulations: application to central and eastern North America. *Bull Seismol Soc Am* 105:1989–2009
- Zeng Y, Petersen M, Boyd O (2022) Lower seismogenic depth model for western US earthquakes. *Seismol Res Lett* 93(6):3186–3204

**Publisher's Note** Springer Nature remains neutral with regard to jurisdictional claims in published maps and institutional affiliations.